AD-A058 784 NAVAL SURFACE WEAPONS CENTER WHITE OAK LAB SILVER SP--ETC F/G 9/5
PERFORMANCE OF POLYMER WAVEGUIDE AT MILLIMETER WAVELENGTHS.(U)
MAY 78 D G JABLONSKI, A M SYELES, A D KRALL

UNCLASSIFIED NSWC/WOL/TR-77-115 NL

1 OF 1
AD
A058 784

END
DATE
FILMED
-11-78
DDC

NSWC/WOL TR-77-115

LEVEL II

12

Final rept.,

PERFORMANCE OF POLYMER WAVEGUIDE AT MILLIMETER WAVELENGTHS

BY D. G. JABLONSKI, A. D. KRALL
A. M. SYELES, O. J. VANSANT

RESEARCH AND TECHNOLOGY DEPARTMENT

MAY 1978

80 p.

Approved for public release; distribution unlimited.

ZR0000 1,
ZR01107

NAVAL SURFACE WEAPONS CENTER

Dahlgren, Virginia 22448 • Silver Spring, Maryland 20910

UNCLASSIFIED

SECURITY CLASSIFICATION OF THIS PAGE (When Data Entered)

REPORT DOCUMENTATION PAGE		READ INSTRUCTIONS BEFORE COMPLETING FORM
1. REPORT NUMBER NSWC/WOL TR 77-115	2. GOVT ACCESSION NO.	3. RECIPIENT'S CATALOG NUMBER
4. TITLE (and Subtitle) PERFORMANCE OF POLYMER WAVEGUIDE AT MILLIMETER WAVELENGTHS		5. TYPE OF REPORT & PERIOD COVERED Final 6. PERFORMING ORG. REPORT NUMBER
7. AUTHOR(s) D. G. Jablonski, A. D. Krall, A. M. Syeles, O. J. VanSant		8. CONTRACT OR GRANT NUMBER(s)
9. PERFORMING ORGANIZATION NAME AND ADDRESS Naval Surface Weapons Center White Oak Silver Spring, Maryland 20910		10. PROGRAM ELEMENT, PROJECT, TASK AREA & WORK UNIT NUMBERS 61152N; ZR00001; ZR01107; WR0173;
11. CONTROLLING OFFICE NAME AND ADDRESS 61152N		12. REPORT DATE May 1978 13. NUMBER OF PAGES 78
14. MONITORING AGENCY NAME & ADDRESS(if different from Controlling Office)		15. SECURITY CLASS. (of this report) UNCLASSIFIED 15a. DECLASSIFICATION/DOWNGRADING SCHEDULE

16. DISTRIBUTION STATEMENT (of this Report)

Approved for public release, distribution unlimited.

17. DISTRIBUTION STATEMENT (of the abstract entered in Block 20, if different from Report)

18. SUPPLEMENTARY NOTES

19. KEY WORDS (Continue on reverse side if necessary and identify by block number)

Millimeter
Dielectric
Waveguide
Polymer

HE11

20. ABSTRACT (Continue on reverse side if necessary and identify by block number)

Investigation and measurements are made at 70 GHz on dielectric waveguide operating in the HE_{11} mode. Loss characteristics radiation, power handling and field characteristics are discussed.

DD FORM 1 JAN 73 1473 EDITION OF 1 NOV 65 IS OBSOLETE
S/N 0102-LF-014-6601

UNCLASSIFIED

SECURITY CLASSIFICATION OF THIS PAGE (When Data Entered)

SUMMARY

At millimeter wave frequencies conventional metal waveguide is extremely lossy and very expensive. Dielectric waveguide may be an inexpensive and practical substitute for many applications.

In this report, we investigate the properties of the hybrid HE_{11} mode of a cylindrical dielectric guide. In particular, the various forms of loss are discussed. Different models are utilized to describe loss due to absorption and scattering, radiation from bends, and radiation due to surface imperfections. A heat transfer model is used to predict the power handling capabilities of a dielectric rod.

To study the performance of an actual dielectric guide, an experiment was done to measure the dielectric constant and attenuation factor of a dielectric rod propagating a single mode at 70 GHz. The attenuation factor is related to an equivalent loss tangent that takes into account all forms of loss. By comparing this loss tangent with available data for the intrinsic tan δ of the dielectric material, one can estimate the relative importance of radiation losses to those due to absorption.

The measurement technique utilizes a long section of dielectric waveguide that can be probed anywhere along its length. The standing wavelength along the rod is easily measured, and leads to a determination of the dielectric constant. Measurement of the average power on the line as a function of position provides the attenuation factor.

Measurements were done using teflon, polystyrene, and fused quartz rods. Dielectric constant at 71.0 GHz was measured for all three materials. The attenuation was measured for several different polystyrene and teflon rods. The results are consistent with published data for the materials at microwave frequencies. In particular, the results indicate that radiation losses may be insignificant.

The report concludes with a summary of the theory of the dielectric waveguide, and a discussion of the problems that remain to be solved before dielectric waveguide will become practical for use with millimeter waves.

An appendix includes numerical calculations of the propagation vector versus rod diameter for different values of ε corresponding to teflon, fused quartz, and polystyrene.

BJ Ubbenga

for PAUL R. WESSEL
By direction

CONTENTS

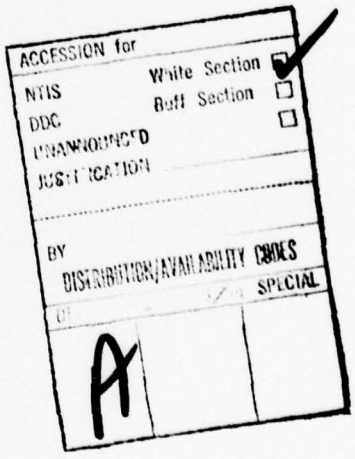

ILLUSTRATIONS

Chapter I

INTRODUCTION

The use of millimeter waves for radar, radiometry, and communications systems is becoming increasingly popular. Because of their small wavelength, millimeter waves provide greater resolution for tracking purposes than do lower frequency microwaves. There is no shortage of possible applications of millimeter waves, but there are a great number of technical problems to be overcome before many of these applications become practical.

Roughly speaking, millimeter waves fall between 30 and 300 GHz. Conventional microwave techniques can be used at the lower end of this spectrum, but they become impractical as the frequency increases. In particular, conventional metal waveguide becomes extremely lossy, and the tolerances required for manufacture cause the cost to be prohibitive. For example, the theoretical attenuation of a rectangular guide at 12 GHz is about .03 dB/ft. At 30 GHz, it is about .15 dB/ft, and at 70 GHz is .5 dB/ft. In practice, the attenuation is about twice as much due to mechanical imperfections and contamination of the conducting surfaces in the guide. There is one notable exception, however. The TE_{01} mode of a cylindrical guide has extremely low loss due to the absence of tangential H field at the walls of the guide. The use of cylindrical metal guide for a long distance communications system is being investigated at Bell Laboratories.[1] In general, the high attenuation makes metal waveguide impractical for many large scale systems. The lack of high power sources at these frequencies only compounds the problem.

There are several alternatives to metal waveguide at millimeter wave frequencies. They include microstrip, strip-line, image line, finline, microguide,

---

1. Abele, T. A. et al, "A High-Capacity Digital Communication System Using TE_{01} Transmission in Circular Waveguide," IEEE Trans. Microwave Theory & Tech., Vol. MTT-23, pp. 326-333, April 1975.

and dielectric waveguide. Dielectric waveguide isn't nearly as sophisticated as the other structures, and it has several drawbacks. Among other things, it doesn't interface with circuitry easily, it can't be etched, and it has poor isolation characteristics.

However, dielectric waveguide merits study because it is so simple and inexpensive. And, in theory, its attenuation can be made arbitrarily small by reducing the dimensions of the guide.

Dielectric waveguide has been the subject of theoretical analysis since 1910, when it was investigated by Hondros and Debye.[2] In recent years, it has been used experimentally for measuring dielectric constants of materials at microwave frequencies.[3] Dielectric waveguide will soon be used in the form of optical fibers for telephone communications, and promises to revolutionize the communications industry.[4]

In this technical report, we investigate the properties of the cylindrical dielectric waveguide at millimeter wave frequencies. The objective is to study the problems that are characteristic of any waveguiding structure in terms of the dielectric cylinder, so that one may develop a basic understanding of the advantages and limitations of any type of structure. The dielectric cylinder is compared with metal waveguide, and with optical fibers when relevant. The discussion is limited primarily to the properties of the HE_{11} mode of the round dielectric guide.

The technical report starts with a discussion of the theories of the lossless dielectric slab and dielectric cylinder. The general solution to Maxwell's equations is derived in terms of a discrete number of guided modes, and an infinite continuum of radiation modes. The cutoff and propagation characteristics of the guided modes are discussed in terms of a guidance condition. Particular emphasis is placed on the properties of the dominant HE_{11} mode of the dielectric cylinder.

---

2. Hondros and Debye, "Electromagnetische Wellen an dielektrischen Drahten," Ann. der Phys., Vol. 32, pp. 465-476, June 1910.
3. Cullen, A. L., and Gillespie, E. F. F., "A New Method for Dielectric Measurements at Millimeter Wavelengths," Presented at the Symposium on Millimeter Waves, Polytechnic Institute of Brooklyn, April 1959.
4. TIME Magazine, Science Section, March 22, 1976.

The effects of loss are introduced using a perturbation technique. The attenuation in a dielectric rod waveguide due to absorption and scattering is described using the theory developed by Elsasser in 1949.[5] The theory of radiation loss from bends and surface imperfections developed by Marcatili and Marcuse at Bell Laboratories is briefly discussed.[6,7,8,9]

To get a practical feel for the problems involved in using a dielectric guide, experimental observations of a cylindrical guide were made at 70 GHz. To verify that the guide was performing in accordance with theory, measurements were made of the dielectric constant and attenuation factor of several teflon, polystyrene, and fused quartz rods. By relating the results to the bulk dielectric constant and loss tangent of the material being used, one can verify that the rod was operating in the HE_{11} mode. In addition, the experimental determination of complex dielectric constant is in itself an important result, as there is not much data available for materials at these frequencies.

Numerical calculations of the propagation characteristics of the HE_{11} mode are included in an appendix.

---

5. Elsasser, W. M., "Attenuation in a Dielectric Circular Rod," J. Appl. Phys. 20, p. 1193, December 1949.
6. Marcatili, E. A. J., "Bends in Optical Dielectric Guides," Bell System Technical Journal, pp. 2103-2132, September 1969.
7. Marcuse, D., and Derosier, R.M., "Mode Conversion Caused by Diameter Changes of a Round Dielectric Waveguide," B.S.T.J. 48, No. 10, pp. 3217-3232, December 1969.
8. Marcuse, D., "Radiation Losses of the Dominant Mode in Round Dielectric Waveguides," B.S.T.J., pp. 1665-1693, October 1970.
9. Marcuse, D., "Radiation Losses of Dielectric Waveguides in Terms of the Power Spectrum of the Wall Distortion Function," B.S.T.J., pp. 3233-3242, December 1969.

Chapter II

THEORY OF THE DIELECTRIC WAVEGUIDE

2.1 THE DIELECTRIC SLAB

To understand the behavior of a dielectric waveguide, it is necessary to solve Maxwell's equations subject to the boundary conditions imposed by the presence of the dielectric. For a non-conducting dielectric in a region where there is no free charge or current, Maxwell's equations are

$$\nabla \times \bar{E} + \frac{\partial \bar{B}}{\partial t} = 0 \qquad (2\text{-}1a) \qquad\qquad \nabla \cdot \bar{B} = 0 \qquad (2\text{-}1c)$$

$$\nabla \times \bar{H} - \frac{\partial \bar{D}}{\partial t} = 0 \qquad (2\text{-}1b) \qquad\qquad \nabla \cdot \bar{D} = 0 \qquad (2\text{-}1d)$$

$$\text{where} \quad \bar{D} = \epsilon \bar{E} \qquad \bar{B} = \mu \bar{H} \qquad (2\text{-}2)$$

To solve the field equations for a dielectric waveguide of uniform cross-section, it is convenient to use the approach developed by Stratton.[10] It is possible to specify both the electric and magnetic fields in terms of a set of Hertz vectors $\bar{\Pi}$ and $\bar{\Pi}^*$, such that

$$\bar{E} = \bar{E}^1 + \bar{E}^2 \qquad (2\text{-}3a) \qquad\qquad \bar{H} = \bar{H}^1 + \bar{H}^2 \qquad (2\text{-}3b)$$

$$\bar{E}^1 = \nabla \times \nabla \times \bar{\Pi} \qquad (2\text{-}4a) \qquad\qquad \bar{H}^1 = \epsilon \nabla \times \frac{\partial \bar{\Pi}}{\partial t} \qquad (2\text{-}4c)$$

$$\bar{E}^2 = -\mu \nabla \times \frac{\partial \bar{\Pi}^*}{\partial t} \qquad (2\text{-}4b) \qquad\qquad \bar{H}^2 = \nabla \times \nabla \times \bar{\Pi}^* \qquad (2\text{-}4d)$$

---

10. Stratton, J. A., Electromagnetic Theory, McGraw-Hill, New York, 1941.

where $\bar{\Pi}$ and $\bar{\Pi}^*$ are specified by

$$\nabla^2\bar{\Pi} - \mu\varepsilon \frac{\partial^2\bar{\Pi}}{\partial t^2} = 0 \qquad (2\text{-}5a) \qquad \nabla^2\bar{\Pi}^* - \mu\varepsilon \frac{\partial^2\bar{\Pi}}{\partial t^2} = 0 \qquad (2\text{-}5b)$$

The vector $\bar{\Pi}$ can be related to the conventional scalar and vector potentials by

$$\Phi = -\nabla \cdot \bar{\Pi} \qquad (2\text{-}6a) \qquad \bar{A} = -\mu\varepsilon \frac{\partial\bar{\Pi}}{\partial t} \qquad (2\text{-}6b)$$

Equations (2-3), (2-4), and (2-5) constitute a general solution to Maxwell's equations in homogeneous, non-conducting media where ρ and $\bar{J}$ are zero.

To describe the behavior of a dielectric waveguide, it is sufficient to find a set of Hertz vectors that are oriented parallel to the axis of the guide. Since these vectors are unidirectional, equations (2-5) become scalar equations. As an illustrative example, consider the slab waveguide of Figure 2-1.

We wish to describe a set of waves, propagating in the z direction, that are guided by the slab. To simplify the discussion, we will treat $\bar{\Pi}$ and $\bar{\Pi}^*$ as being dimensionless. The mathematics will be unchanged, and appropriate scaling factors can always be added to the final solution. Let $\bar{\Pi} = \bar{\Pi}^* = \psi\hat{z}$. Then (2-5) becomes

$$\nabla^2\psi - \mu\varepsilon \frac{\partial^2\psi}{\partial t^2} = 0 \qquad (2\text{-}7)$$

Since ε is different in the two regions $|x| \leq d$ and $|x| > d$, it will be necessary to solve (2-7) in each of the regions using the proper value of ε.

Since we are interested in time-harmonic waves propagating in the z direction, let

$$\psi = f(x,y)e^{\pm ihz - i\omega t} \qquad (2\text{-}8)$$

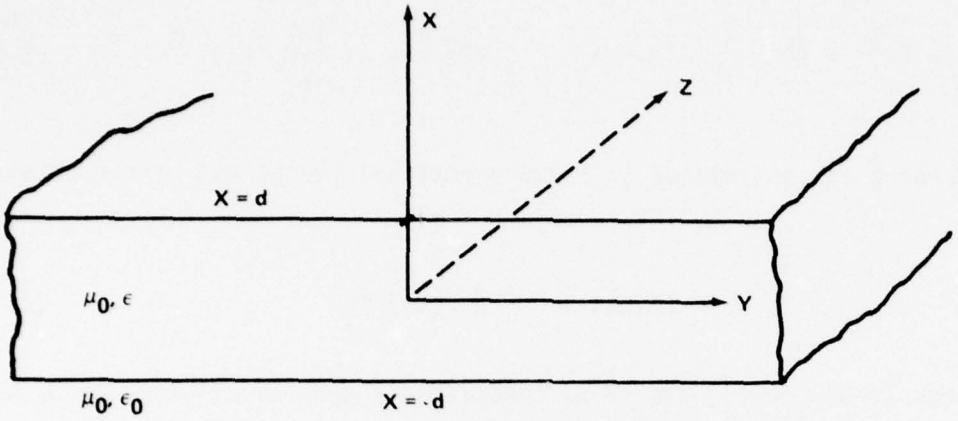

FIG. 2-1 DIELECTRIC SLAB WAVEGUIDE

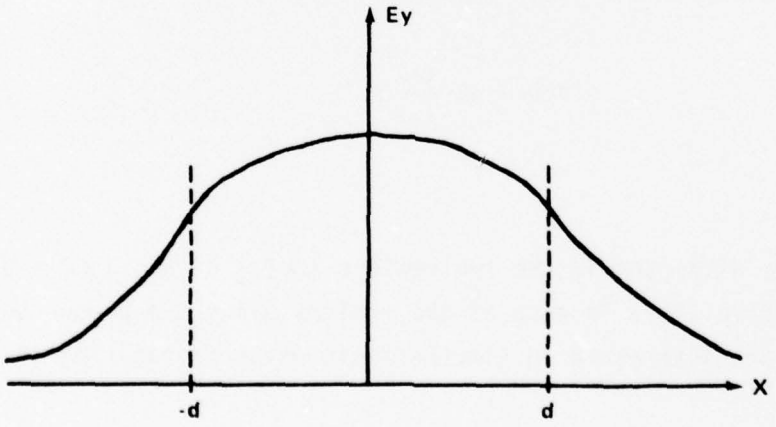

FIG. 2-2 FIELD PROFILE OF A WAVE ON A DIELECTRIC SLAB

Expressing equations (2-4) in a Cartesian system and making use of (2-8), we get

$$E_x^1 = \pm ih \frac{\partial \psi}{\partial x} \qquad E_y^1 = \pm ih \frac{\partial \psi}{\partial y} \qquad E_z^1 = (k^2 - h^2)\psi \tag{2-9a}$$

$$H_x^1 = -\frac{ik^2}{\mu\omega} \frac{\partial \psi}{\partial y} \qquad H_y^1 = \frac{ik^2}{\mu\omega} \frac{\partial \psi}{\partial y} \qquad H_z^1 = 0 \tag{2-9b}$$

$$E_x^2 = i\mu\omega \frac{\partial \psi}{\partial y} \qquad E_y^2 = -i\mu\omega \frac{\partial \psi}{\partial x} \qquad E_z^2 = 0 \tag{2-10a}$$

$$H_x^2 = \pm ih \frac{\partial \psi}{\partial y} \qquad H_y^2 = \pm ih \frac{\partial \psi}{\partial y} \qquad H_z^2 = (k^2 - h^2)\psi \tag{2-10b}$$

where $k = \omega\sqrt{\mu\varepsilon}$, and

$$\frac{\partial^2 \psi}{\partial x^2} + \frac{\partial^2 \psi}{\partial y^2} + (k^2 - h^2)\psi = 0 \tag{2-11}$$

and $\bar{E} = \bar{E}^1 + \bar{E}^2$, $\bar{H} = \bar{H}^1 + \bar{H}^2$.

The significance of this approach can be seen from equations (2-9), (2-10), and (2-11). By solving a single scalar homogeneous wave equation, we are able to find the general solution for the electric and magnetic fields of a dielectric waveguide. Furthermore, the solutions are conveniently separated into TE and TM waves. (In general, there is no TEM solution for a dielectric guide, due to the impossibility of satisfying all of the boundary conditions simultaneously.)

To continue the analysis of the dielectric slab, solve equation (2-11) and impose the boundary conditions that tangential E and H are continuous at the surface of the slab. To simplify the analysis, let us restrict the solution to be transverse electric (TE) and to be independent of y (i.e. - $\partial/\partial y = 0$). Making use of equation (2-8), equation (2-11) becomes

$$\frac{\partial^2 f(x)}{\partial x^2} + (k^2 - h^2) f(x) = 0 \qquad (2\text{-}12)$$

and has the solutions

$$f(x) = \begin{bmatrix} \sin\beta x & e^{-\gamma x} \\ \cos\beta x & e^{\gamma x} \end{bmatrix} \qquad (2\text{-}13)$$

where

$$\beta = \sqrt{k^2 - h^2} \qquad \gamma = \sqrt{h^2 - k^2} \qquad (2\text{-}14)$$

To describe a guided mode, we would like the fields to decay with increasing x, so that there is no electromagnetic radiation at large distances from the slab. Therefore we let

$$f(x) = \begin{bmatrix} Ae^{-\gamma x} & x > d \\ Ae^{+\gamma x} & x < -d \\ B\sin\beta x & |x| < d \end{bmatrix} \qquad (2\text{-}15)$$

The fields are

$x < -d$	$\lvert x\rvert \leq d$	$x > d$
$E_y = -i\mu\omega\gamma Ae^{\gamma x}$	$E_y = -i\mu\omega\beta B\cos\beta x$	$E_y = i\mu\omega\gamma Ae^{-\gamma x}$
$H_z = -\gamma^2 Ae^{\gamma x}$	$H_z = \beta^2 B\sin\beta x$	$H_z = -\gamma^2 Ae^{-\gamma x}$
$H_x = \pm ih\gamma Ae^{\gamma x}$	$H_x = \pm ih\beta B\cos\beta x$	$H_x = \pm ih\gamma Ae^{-\gamma x}$

(2-16)

where $\exp\{\pm ihz - i\omega t\}$ is understood.

Matching tangential E and H at x = d,

$$\beta B\cos\beta d = -\gamma A e^{-\gamma d} \tag{2-17a}$$

$$\beta^2 B\sin\beta d = -\gamma^2 A e^{-\gamma d} \tag{2-17b}$$

Dividing (2-17b) by (2-17a) yields

$$\tan\beta d = \gamma/\beta \tag{2-18}$$

where γ and β are functions of h defined by (2-14).

Equation (2-18) is the guidance condition that determines the eigenvalues h, the propagation constant in the z direction. Since the tangent function is periodic, there are numerous values of h, each corresponding to a different TE waveguide mode. In general

$$\omega\sqrt{\mu_o\varepsilon_o} < h < \omega\sqrt{\mu_o\varepsilon} \tag{2-19}$$

In terms of the phase velocity ω/k, this means that a wave travels fastest in free space where $\varepsilon = \varepsilon_o$. But a wave propagating along a dielectric guide moves faster than a wave traveling through an infinite dielectric. Each of the guided modes propagates with a different phase velocity.

By renormalizing E_y, we have

$$\begin{aligned} E_y &= A\cos\beta x && |x| \leq d \\ E_y &= A\cos\beta d\, e^{-\gamma(x-d)} && x > d \\ E_y &= A\cos\beta d\, e^{+\gamma(x-d)} && x < -d \end{aligned} \tag{2-20}$$

The field profile for the lowest order mode as a function of x is sketched in Figure 2-2. The important thing to notice is that the fields evanesce outside the slab. This means that no energy is lost to radiation at large distances from the slab. However, a substantial portion of the energy is propagating outside the slab.

Instead of choosing fields that decay with increasing x, we could let

$$f(x) = Ae^{i\rho x} + Be^{-i\rho x} \tag{2-21a}$$

outside of the slab, and

$$f(x) = C\sin\sigma x \tag{2-21b}$$

inside the slab. Repeating the analysis, this leads to

$$E_y = Ae^{i\rho x} + Be^{-i\rho x} \tag{2-22a}$$

$$E_y = C\cos\sigma x \tag{2-22b}$$

where A, B, and C have been renormalized, and

$$\sigma = (\omega^2\mu_o\varepsilon - h^2)^{1/2} \qquad \rho = (\omega^2\mu_o\varepsilon_o - h^2)^{1/2} \tag{2-23}$$

The propagation constant ρ can assume any value. Unlike the previous example where h is a discrete eigenvalue determined by (2-18), h can now have any value in the range

$$0 \leq h \leq \omega\sqrt{\mu_o\varepsilon_o} \tag{2-24}$$

In general, there are two sets of solutions for the fields of a dielectric waveguide. The first set includes all guided, or bound modes, which are a finite set of waves characterized by discrete values of the propagation constant h. These modes evanesce outside the guide and do not radiate. The constant h is determined by a transcendental equation such as (2-18).

The second set of solutions is comprised of the radiation modes, or modes of the continuum.[11] They are infinite in number, and can be described as incident waves that are reflected at the dielectric in such a way that all boundary conditions are satisfied. The value of h is now continuously variable, and does not depend on a transcendental equation.

11. Marcuse, D., "Mode Conversion Caused by Surface Imperfections of a Dielectric Slab Waveguide," B.S.T.J. 48, No. 10, pp. 3177-3215, December 1969.

The guided and radiation modes are analogous to the quantum mechanical solution for the wavefunctions of an electron in a potential well. The guided modes or radiation modes, correspond to free electrons, which can have any energy.

This analogy isn't as farfetched as it seems. For example, it can be shown that the angular momentum per unit energy for a guided mode on a dielectric cylinder is quantized in units of -nh´, where n is an integer and h´ is Planck's constant divided by 2π.[12] However, the subject of quantized fields is not essential to the understanding of dielectric waveguide and will not be considered here.

Under appropriate conditions, the guided and radiation modes of the dielectric waveguide can couple. However, for a perfectly uniform and lossless guide with no bends or surface imperfections, the modes will not interact.

2.2 THE DIELECTRIC CYLINDER

The boundary value problem of the cylindrical guide has been solved by several authors. The derivation presented here follows Stratton, and utilizes the same approach that was used for the dielectric slab of section 2.1.[10] However, here we will find a guidance condition that describes all of the modes, rather than limiting the argument to a specific type of mode (i.e., TE or TM).

Consider the dielectric cylinder of Figure 2-3. The cylinder has dielectric constant ε_1 and permeability μ_1. The surrounding medium is characterized by $\varepsilon = \varepsilon_2$ and $\mu = \mu_2$. The radius of the cylinder is a.

We can define a Hertz vector $\overline{\Pi} = \overline{\Pi}^* = \psi\hat{z}$, where

$$\psi = f(r,\theta)e^{\pm ihz - i\omega t} \tag{2-25}$$

Equations (2-5a) and (2-5b) are now identical and become

$$\frac{1}{r}\frac{\partial}{\partial r}\left[r\frac{\partial f}{\partial r}\right] + \frac{1}{r}\frac{\partial^2}{\partial\theta^2} + (k^2 - h^2)f = 0 \tag{2-26}$$

Using a separation of variables technique, let $f(r,\theta) = f_1(r)f_2(\theta)$. Then

---

10. Stratton, J. A., Electromagnetic Theory, McGraw-Hill, New York, 1941.
12. Kapany, N.S., and Burke, J.J., Optical Waveguides, Academic Press, New York, 1972, p. 96.

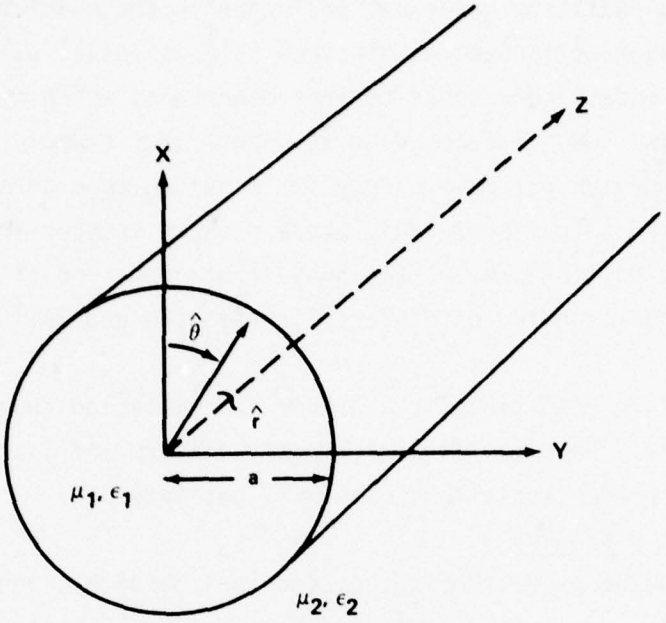

FIG. 2-3 DIELECTRIC CYLINDER

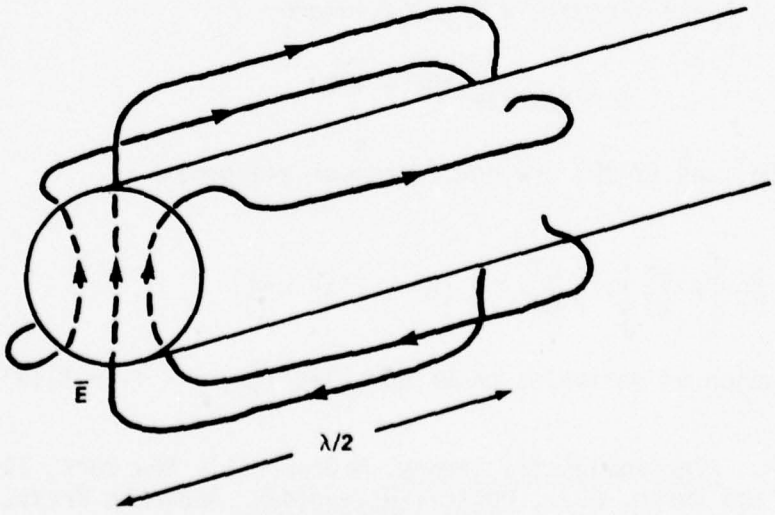

FIG. 2-4 HE_{11} MODE OF THE DIELECTRIC CYLINDER

$$r \frac{d}{dr}\left(r \frac{df_1}{dr}\right) + \left((k^2 - h^2)r^2 - p^2\right) f_1 = 0 \qquad (2\text{-}27)$$

$$\frac{d^2 f_2}{d\theta^2} + p^2 f_2 = 0 \qquad (2\text{-}28)$$

where p is a separation constant. Equation (2-28) is Bessel's equation, and has solutions

$$f_1(r) = Z_p(\sqrt{k^2 - h^2}\, r) \qquad (2\text{-}29)$$

where Z_p can be any of the following

$J_p(\lambda r)$	Bessel function	(2-30)
$N_p(\lambda r)$	Neumann function	(2-31)
$H_p^1(\lambda r)$	Hankel function of first kind	(2-32)
$H_p^2(\lambda r)$	Hankel function of second kind	(2-33)

where $\lambda = (k^2 - h^2)^{\frac{1}{2}}$.

Equation (2-28) is the wave equation and has solutions of the form

$$f_2(\theta) = e^{ip\theta} \qquad (2\text{-}34)$$

The general solution for ψ can be expressed as

$$\psi_n = e^{in\theta} Z_n (\sqrt{k^2 - h^2}\, r) e^{\pm ihz - i\omega t} \tag{2-35}$$

where the constant h is determined by applying the boundary conditions at the surface of the cylinder to appropriate solutions of Z_n.

From the relationships (2-4) we have

$$\bar{E}^1 = \nabla \times \nabla \times \psi\hat{z} \tag{2-36a}$$

$$\bar{E}^2 = -\mu\frac{\partial}{\partial t}\nabla \times \psi\hat{z} \tag{2-36b}$$

$$\bar{H}^1 = \epsilon\frac{\partial}{\partial t}\nabla \times \psi\hat{z} \tag{2-36c}$$

$$\bar{H}^2 = \nabla \times \nabla \times \psi\hat{z} \tag{2-36d}$$

In a cylindrical coordinate system, equations (2-36) reduce to

$$E_r^1 = \pm ih\frac{\partial\psi}{\partial r} \qquad E_\theta^1 = \pm\frac{ih\partial\psi}{r\partial\theta} \qquad E_z^1 = (k^2 - h^2)\psi \tag{2-37a}$$

$$H_r^1 = -\frac{ik^2\partial\psi}{\mu\omega r\partial\theta} \qquad H_\theta^1 = \frac{ik^2\partial\psi}{\mu\omega\partial r} \qquad H_z^1 = 0 \tag{2-37b}$$

$$E_r^2 = \frac{i\mu\omega\partial\psi}{r\partial\theta} \qquad E_\theta^2 = -i\mu\omega\frac{\partial\psi}{\partial r} \qquad E_z^2 = 0 \tag{2-38a}$$

$$H_r^1 = \pm ih\frac{\partial\psi}{\partial r} \qquad H_\theta^2 = \pm\frac{ih\partial\psi}{r\partial\theta} \qquad H_z^2 = (k^2 - h^2)\psi \tag{2-38b}$$

Note that the solutions are again broken up into TE and TM solutions, as they were for the slab waveguide. Also note that $\partial\psi_n/\partial\theta = in\psi_n$. In order for the fields to be single-valued functions of θ, it is necessary for n to be an integer. Since this is the case, it is possible to write the general solution for the fields as a summation over the mode index n from $n = -\infty$ to ∞. The mode amplitudes are a_n for the TM components and b_n for the TE components. The general solutions for the electric field are

$$E_r = ih \sum a_n \frac{\partial \psi_n}{\partial r} - \frac{\mu\omega}{r} \sum n b_n \psi_n \tag{2-39a}$$

$$E_\theta = -\frac{h}{r} \sum n a_n \psi_n - i\mu\omega \sum b_n \frac{\partial \psi_n}{\partial r} \tag{2-39b}$$

$$E_z = (k^2 - h^2) \sum a_n \psi_n \tag{2-39c}$$

where all of the summations are from $n = -\infty$ to ∞. The equations for the magnetic field are similar.

These equations are the starting place for the analysis of optical fibers, and are referred to in many journal articles.

To solve for the fields of the dielectric cylinder, we must choose appropriate forms for ψ_n in each of two regions, $r < a$ and $r > a$. Then we must use the boundary conditions to match the solutions at $r = a$. For a satisfactory solution, the fields E and H must decay for large r, and be finite on the axis. To insure this, let

$$\psi_n = J_n(\sqrt{k^2 - h^2}\, r) \tag{2-40}$$

for $r \leq a$

and

$$\psi_n = H_n^1(\sqrt{k^2 - h^2}\, r) \tag{2-41}$$

for $r > a$

The Bessel function is finite at $r = 0$, and the Hankel function of the first kind decays for large values of r. It is convenient to keep Stratton's notation and define

$$k = k_1 = \omega\sqrt{\mu_1\varepsilon_1} \tag{2-42a}$$

inside the cylinder

$$k = k_2 = \omega\sqrt{\mu_2\varepsilon_2} \tag{2-42b}$$

outside the cylinder

For $r < a$, the z components of the fields are

$$E_z^i = \sum_n [J_n(\lambda_1 r)a_n^i]F_n \tag{2-43a}$$

$$H_z^i = \sum_n [J_n(\lambda_1 r)b_n^i]F_n \tag{2-43b}$$

and for $r > a$,

$$E_z^e = \sum [H_n^1(\lambda_2 r)a_n^e]F_n \tag{2-44a}$$

$$H_z^e = \sum [H_n^1(\lambda_2 r)b_n^e]F_n \tag{2-44b}$$

where $\lambda_1^2 = k_1^2 - h^2$, $\lambda_2^2 = k_2^2 - h^2$, and

$$F_n = \exp\{in\theta + ihz - i\omega t\} \tag{2-45}$$

The r and θ components can be derived in a similar manner.

The boundary conditions are that tangential E and H must be continuous at $r = a$. Matching the z components of E and H yields

$$J_n(u)a_n^i = H_n^1(v)a_n^e \tag{2-46a}$$

$$J_n(u)b_n^i = H_n^1(v)b_n^e \tag{2-46b}$$

The θ components are matched in the same way. However, the expressions are more complicated. We get

$$\frac{nh}{u^2} J_n(u)a_n^i + \frac{i\mu_1\omega}{u} J_n'(u)b_n^i = \frac{nh}{v^2} H_n^1(v)a_n^e + \frac{i\mu_2\omega}{v} H_n^{1\prime}(v)b_n^e \tag{2-47a}$$

$$\frac{ik_1^2}{\mu_1\omega u} J_n'(u)a_n^i - \frac{nh}{u^2} J_n(u)b_n^i = \frac{ik_2^2}{\mu_2\omega v} H_n^{1\prime}(v)a_n^e - \frac{nh}{v^2} H_n^1(v)b_n^e \tag{2-47b}$$

$$u = \lambda_1 a \qquad v = \lambda_2 a \tag{2-48}$$

The presence of a prime denotes differentiation with respect to the argument of the function.

The set of equations (2-46) and (2-47) are a linear system of equations that are satisfied by the mode coefficients a_n^i, b_n^i, a_n^e, and b_n^e. To have a nontrivial solution, their determinant must be zero. This gives the guidance condition for the dielectric rod.

$$\left[\frac{\mu_1}{u}\frac{J_n'(u)}{J_n(u)} - \frac{\mu_2}{v}\frac{H_n'(v)}{H_n(v)}\right]\left[\frac{k_1^2}{\mu_1 u}\frac{J_n'(u)}{J_n(u)} - \frac{k_2^2}{\mu_2 v}\frac{H_n'(v)}{H_n(v)}\right] = n^2h^2\Omega \tag{2-49}$$

where $\Omega = (1/v^2) - (1/u^2)$, and the superscript ^{1} has been deleted from the Hankel functions of the first kind.

This transcendental equation determines the mode propagation constant h.

Referring to equations (2-46), (2-47), and (2-49), there are several significant observations that can be made. If either the set of coefficients a_n or b_n are arbitrarily set to zero, then the equations have no solution except for the case $n = 0$. This means that for $n \neq 0$, only hybrid solutions with both $E_z \neq 0$ and $H_z \neq 0$ are allowed. Because of this hybrid nature, modes are described by the notation EH_{nm} and HE_{nm}, depending on whether TE or TM waves dominate the solution.[13] The subscript n refers to the order of the wavefunction. For each value of n, there is an infinite number of roots for the propagation constant h. These roots are designated by the subscript m, where m is related to the number of nulls in the field pattern.

For n = 0, the guidance condition reduces to two independent equations. These are

$$\frac{\mu_1}{u}\frac{J_1(u)}{J_0(u)} = \frac{\mu_2}{v}\frac{H_1^1(v)}{H_0^1(v)} \tag{2-50}$$

and

$$\frac{k_1^2}{\mu_1 u}\frac{J_1(u)}{J_0(u)} = \frac{k_2^2}{\mu_2 v}\frac{H_1^1(v)}{H_0^1(v)} \tag{2-51}$$

where the relationships $J_0'(u) = J_1(u)$ and $H_0'(v) = H_1(v)$ have been used.

From equations (2-47) with n = 0, it can be seen that a_0 and b_0, the mode coefficients for the n = 0 mode, are independent of each other. In addition, the fields have no θ dependence. Equation (2-50) describes the EH_{0m} modes, which are transverse electric and are also designated as TE_{0m}. Equation (2-51) describes the HE_{0m} modes, which are transverse magnetic and are designated as TM_{0m}. Unlike the higher modes, which are hybrid in nature, the TE_{0m} and TM_{0m} modes can exist independently of each other.

13. Ibid, p. 118.

The simplest n = 1 modes are the EH_{11} and HE_{11} modes, which for our purposes can be considered identical. These modes have a unique property that can be seen by investigating the behavior of the propagation constant h as the rod diameter is decreased.

For a dielectric rod that is infinite in diameter, all of the modes will propagate. As the diameter is decreased, the values of h corresponding to higher order modes become imaginary, and the modes are cut off. For a sufficiently small radius, only the TE_{01}, TM_{01}, and HE_{11} modes will propagate. There is a critical radius below which even the TE_{01} and TM_{01} modes will be cut off. However, the HE_{11} mode has no cutoff, and in theory can propagate on an infinitesimally small rod. For this reason, the HE_{11} mode is called the dominant mode. It is also referred to sometimes as the dipole mode.

The critical radius below which all modes except the HE_{11} mode are cut off is given by[14]

$$J_0(x) = 0 \tag{2-52a}$$

$$x = 2\pi a(\varepsilon_r - 1)^{\frac{1}{2}}/\lambda_0 \tag{2-52b}$$

where a is the critical radius

λ_0 is the free space wavelength of the propagating wave

ε_r is the relative dielectric constant $\varepsilon_2/\varepsilon_1$

In this report, we will consider only dielectric rods smaller than this critical diameter. We will be concerned only with the propagation characteristics of the dominant HE_{11} mode. The field pattern of the HE_{11} mode is sketched in Figure 2-4.

---

14. Ibid, p. 150.

The experimental analysis will be based on a dielectric rod suspended in air. Thus we can let

$$\mu_1 = \mu_2 = \mu_0 \tag{2-53a}$$

$$\varepsilon_2 = \varepsilon_0 \tag{2-53b}$$

$$k_2 = \omega(\mu_0\varepsilon_0)^{\frac{1}{2}} = 2\pi/\lambda_0 \tag{2-53c}$$

$$k_1 = \omega(\mu_1\varepsilon_1)^{\frac{1}{2}} = 2\pi/\lambda_1 \tag{2-53d}$$

where λ_0 is the free space wavelength, and λ_1 is the wavelength we would expect if the dielectric medium ε_1 extended infinitely in all directions.

It is convenient to let h, the propagation constant along the axis of the rod, be defined as

$$h = 2\pi/\lambda \tag{2-53e}$$

where λ without a subscript refers to the characteristic wavelength of a wave propagating down the rod.

The guidance condition for the HE_{11} mode is plotted in Figure 2-5 as a function of λ/λ_0 and rod diameter. It is plotted for three values of dielectric constant corresponding to fused quartz, polystyrene, and teflon. From the figure, it can be seen that the phase velocity approaches the limiting value of $c/(\varepsilon_r^{\frac{1}{2}})$, where $\varepsilon_r = \varepsilon/\varepsilon_0$, and c is the speed of light.

We have not solved for the radiation modes of the dielectric cylinder. These modes are derived from solutions for ψ_n that do not decay for large r (such as the Neumann functions). However, instead of being plane waves, as was the case for the dielectric slab, the radiation modes will be a superposition of cylindrical waves. The radiation modes of the dielectric cylinder are discussed in more detail by Marcuse.[15]

15. Marcuse, D., "Radiation Losses of the Dominant Mode in Round Dielectric Waveguides," B.S.T.J., pp. 1665-1693, October 1970.

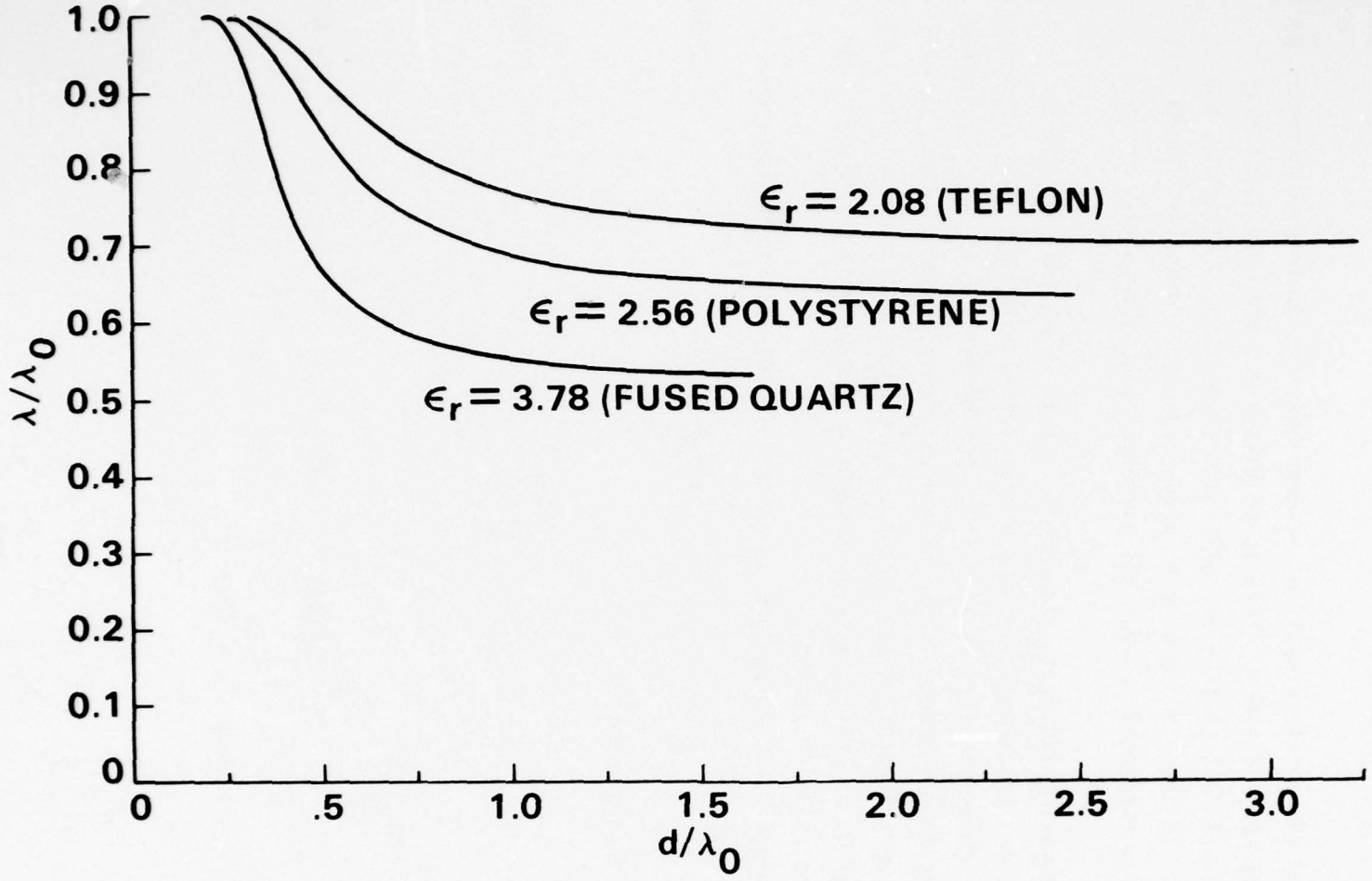

Fig. 2-5 Propagation Characteristics of the HE_{11} Mode

2.3 ATTENUATION

The theory of the previous sections assumed that the dielectric material and surrounding medium were lossless. This is certainly not the case for a real structure. An actual dielectric guide will have absorption, scattering, and radiation losses. If the rod diameter is above the cutoff diameter, there will also be some energy exchanged between the different modes, resulting in mode conversion loss.

To make an experimental evaluation of dielectric waveguide, it will be necessary to measure the attenuation, and where possible, to determine its source. To model the loss theoretically, we will treat the effects of loss as a perturbation to the propagation characteristics of the HE_{11} mode. Specifically, we will assume that the mode propagation constant h is unchanged. All forms of loss will be lumped together as an equivalent loss tangent of the material, and will lead to an effective attenuation factor α.

Consider a plane wave propagating in an infinite dielectric medium where

$$\mu = \mu_0 \qquad \varepsilon = \varepsilon' - i\varepsilon'' \tag{2-54}$$

The wave is determined by

$$\frac{\partial^2 E}{\partial t^2} = \frac{1}{\mu\varepsilon}\frac{\partial^2 E}{\partial t^2} \tag{2-55}$$

E will be of the form

$$E = E_0 \exp(\pm\gamma z - i\omega t) \tag{2-56}$$

where $\gamma^2 = -\omega^2\mu\varepsilon$. Letting $\gamma = \alpha + i\beta$,

$$\alpha^2 - \beta^2 + 2i\alpha\beta = -\omega^2\mu\varepsilon' + i\omega^2\mu\varepsilon'' \tag{2-57}$$

Assuming low loss, $\alpha << \beta$ and $\varepsilon'' << \varepsilon'$, we get

$$\beta \simeq \omega\sqrt{\mu\varepsilon'} \qquad 2\alpha \simeq \omega\sqrt{\mu\varepsilon'}\,(\varepsilon''/\varepsilon') \tag{2-58}$$

Defining $\varepsilon/\varepsilon_0 = \varepsilon_r$, and $\varepsilon''/\varepsilon' = \tan\delta$, and assuming $\varepsilon' \simeq \varepsilon$, equation (2-58) becomes

$$2\alpha \simeq \omega\sqrt{\mu_0\varepsilon_0}\sqrt{\varepsilon_r}\ \tan\delta \tag{2-59}$$

$\omega\sqrt{\mu_0\varepsilon_0}$ is the free space wavevector, and

$$\omega\sqrt{\mu_0\varepsilon_0} = 2\pi/\lambda_0 \tag{2-60}$$

The final result is

$$2\alpha \simeq (2\pi/\lambda_0)\sqrt{\varepsilon_r}\ \tan\delta \tag{2-61}$$

where

$$E = E_0\exp\{-\alpha z \pm i\beta z - i\omega t\} \tag{2-61}$$

α is the voltage attenuation per unit length, and 2α is the power attenuation per unit length.

We can relate this to the round dielectric guide by equating β with h. However, the attenuation factor α was derived by assuming that the dielectric medium extended infinitely in all directions. In the case of a dielectric guide, part of the power is propagating outside of the guide and won't be directly attenuated by the dielectric. But since the field strength outside the guide is determined by the field strength inside the guide, power loss within the dielectric will result in attenuation of both the internal and external fields. One can take this into account by applying Poynting's Theorem. Consider the section of waveguide in Figure 2-6. If all of the power is propagating in the direction of the

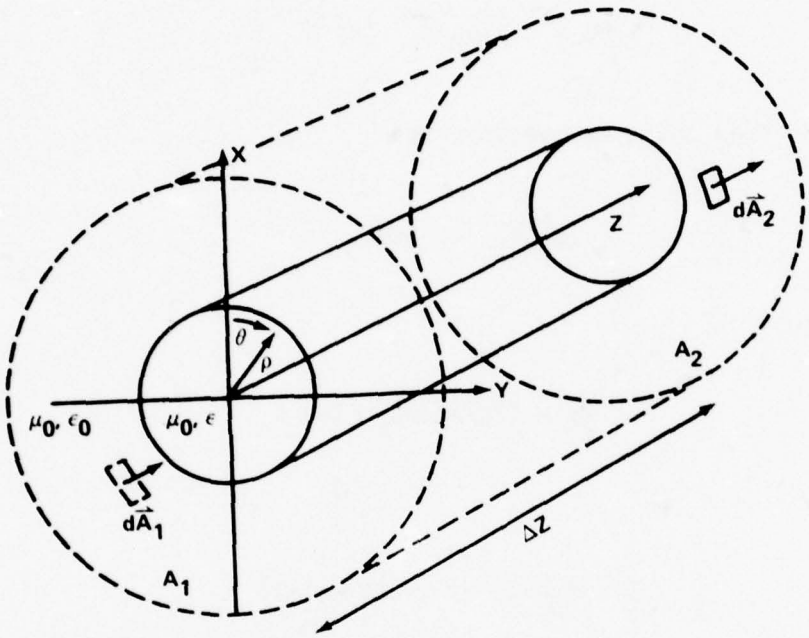

$$d\vec{A}_1 = \rho d\rho d\theta \hat{z}$$

$$\vec{E} \times \vec{H},\ d\vec{A} = (E_\rho H_\theta - E_\theta H_\rho)$$

$$\vec{E} \cdot \vec{J} = r(E_\rho E_\rho + E_\theta E_\theta + E_z E_z)$$

FIG. 2-6 SECTION OF DIELECTRIC WAVEGUIDE

rod, then the net power flow into the volume element dV is

$$P_{in} = \int \bar{E} \times \bar{H} \cdot d\bar{A}_1 \tag{2-62a}$$

The power leaving the volume is

$$P_{out} = \int \bar{E} \times \bar{H} \cdot d\bar{A}_2 \tag{2-62b}$$

The energy dissipated is

$$\int \bar{E} \cdot \bar{J}\, dV, \text{ where } \bar{J} = \sigma \bar{E} \tag{2-62c}$$

(σ need not be an Ohmic conductivity; in the case of a lossy dielectric, $\sigma = \omega\varepsilon \tan \delta$.)

Conservation of power requires that

$$\int \bar{E} \times \bar{H} \cdot d\bar{A}_1 - \int \bar{E} \times \bar{H} \cdot d\bar{A}_2 = \int \bar{E} \cdot \bar{J}\, dV \tag{2-62d}$$

Defining $\Phi = \int \bar{E} \times \bar{H} \cdot d\bar{A}$, and taking the limit as $\Delta z \to 0$, equation 2-62d becomes

$$\frac{d\Phi}{dz} = \int \bar{E} \cdot \bar{J}\, dA \tag{2-62e}$$

Redefining α to be the power attenuation factor (as opposed to voltage attenuation), we have

$$\alpha = \frac{1}{\Phi} \frac{d\Phi}{dz} \tag{2-63a}$$

This leaves

$$\alpha = \frac{\int \bar{E} \cdot \bar{J}\, dA}{\int \bar{E} \times \bar{H} \cdot d\bar{A}} = \frac{\int_0^{2\pi} \int_0^{\infty} \bar{E} \cdot \bar{J}\, \rho d\rho d\theta}{\int_0^{2\pi} \int_0^{\infty} E_\rho H_\theta - E_\theta H_\rho\, \rho d\rho d\theta} \tag{2-63b}$$

If the medium outside the dielectric is lossless, the current density $\bar{J}$ will be zero for $\rho > a$. Thus the integral in the numerator need only be evaluated between $0 < \rho < a$.

By introducing the free space impedance $\eta_0 = \sqrt{\mu_0/\varepsilon_0}$, and relating the conductivity σ to the loss tangent of the dielectric, equation 2-63b can be rewritten

$$\alpha = \sigma\eta R = \varepsilon_r \tan\delta\ \omega\sqrt{\mu_0\varepsilon_0}R = \frac{2\pi}{\lambda_0}\ \varepsilon_r \tan\delta\ R \tag{2-64a}$$

where

$$R = \frac{\int_0^{2\pi}\int_0^{a} |\bar{E}|^2/\eta_0 \rho d\rho d\theta}{\int_0^{2\pi}\int_0^{\infty} E_\rho H_\theta - E_\theta H_\rho\ \rho d\rho d\theta} \tag{2-64b}$$

R can be calculated for the HE_{11} mode from the following equations.[16]

$$R = \left| \frac{\frac{\varepsilon - 1}{q^2}\ \frac{f^2 + (1/p^2) - (1/p^4)}{(1/p^2) + (1/q^2)} + (U^2 + V^2)X + \frac{4UV}{p^4}}{UX(\varepsilon + V^2) + UY(1 + V^2) + \frac{2V}{p^4}(\varepsilon + U^2) - \frac{2V}{q^4}(1 + U^2)} \right| \tag{2-65}$$

$$\{(p^2 + q^2)/(\varepsilon - 1)\}^{\frac{1}{2}} = (2\pi a/\lambda_0) \tag{2-66}$$

$$U = \lambda_0/\lambda = \{(\varepsilon q^2 + p^2)/(q^2 + p^2)\}^{\frac{1}{2}} \tag{2-67}$$

$$V = \{(\varepsilon f + g)/(f + g)\}^{\frac{1}{2}} \tag{2-68}$$

$$X = f^2 + (2f + 1)/p^2 - 1/p^4 \tag{2-69}$$

16. Elsasser, W. M., "Attenuation in a Dielectric Circular Rod," J. Appl. Phys. 20, p. 1193, December 1949.

$$Y = -g^2 - (2g - 1)/q^2 + 1/q^4 \qquad (2\text{-}70)$$

$$f = \frac{J_n'(p)}{pJ_n(p)} \qquad g = \frac{H_n^{2\prime}(q)}{qH_n^2(q)} \qquad (2\text{-}71)$$

The significance of equations (2-65) through (2-71) is that we can relate the observed attenuation factor of a dielectric rod to the bulk loss tangent of the dielectric material.

In practice, R is found by measuring the rod diameter, the guide wavelength λ, and the free space wavelength λ_0. This allows one to calculate ϵ from the guidance condition (2-49), after which the remaining equations can be solved. The attenuation in a dielectric cylinder is directly proportional to R. R as a function of rod diameter is plotted in Figure 2-7 for polystyrene with a loss tangent of .001.

2.4 RADIATION LOSS

Although it is a critical issue, the problem of radiation from bends and surface imperfections is very complicated, and only a basic outline of the problem will be presented here. This disucssion is based on the work of Marcatili and Marcuse at Bell Laboratories.[6,7,8,9] They are principally concerned with optical fibers, but their theories are general and apply at millimeter wave frequencies. In fact, Marcuse and Marcatili have verified some of their ideas experimentally using teflon rods at 55 GHz.[7]

---

6. Marcatili, E. A. J., "Bends in Optical Dielectric Guides," Bell System Technical Journal, pp. 2103-2132, September 1969.
7. Marcuse, D., and Derosier, R.M., "Mode Conversion Caused by Diameter Changes of a Round Dielectric Waveguide," B.S.T.J. 48, No. 10, pp. 3217-3232, December 1969.
8. Marcuse, D., "Radiation Losses of the Dominant Mode in Round Dielectric Waveguides," B.S.T.J., pp. 1665-1693, October 1970.
9. Marcuse, D., "Radiation Losses of Dielectric Waveguides in Terms of the Power Spectrum of the Wall Distortion Function," B.S.T.J., pp. 3233-3242, December 1969.

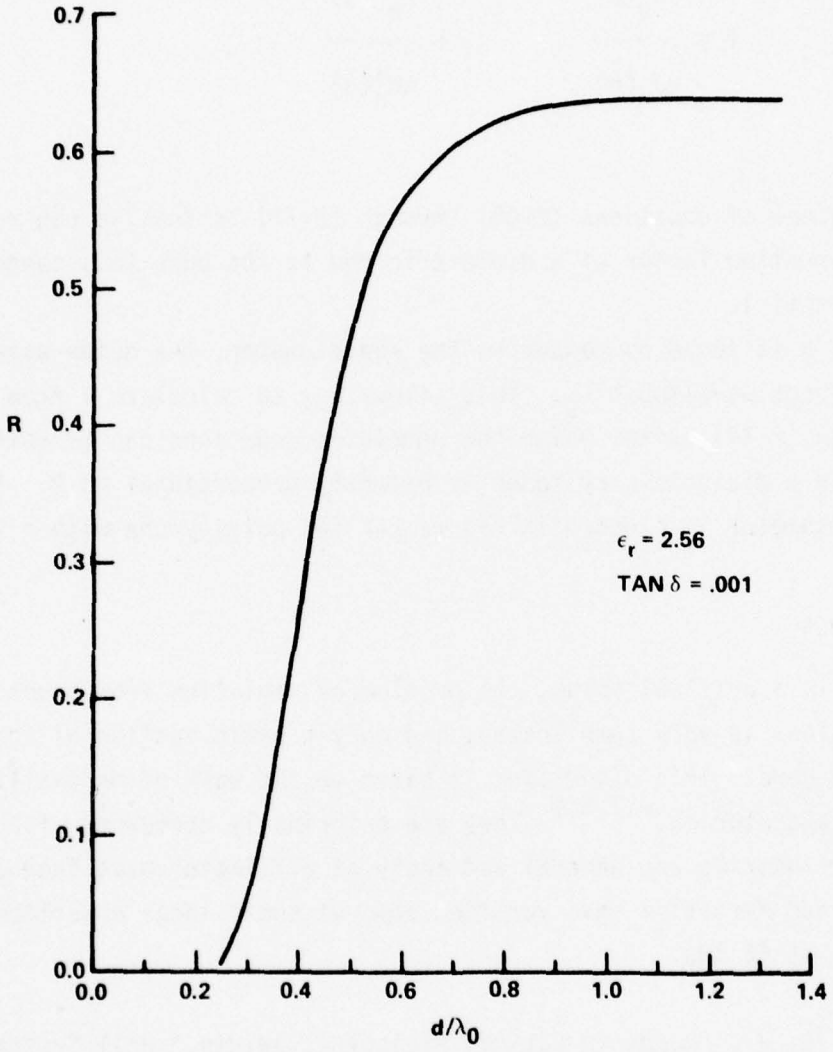

FIG. 2-7 ATTENUATION FACTOR AS A FUNCTION OF ROD DIAMETER (AFTER ELSASSER[16])

Radiation can be caused either by surface imperfections or bends in the dielectric rod. Mathematically, a bend is just the limiting case of a very long surface imperfection. The mechanism for radiation is the coupling of the discrete, guided modes to the continuous, unguided modes. This occurs at surface imperfections and bends due to the impossibility of matching all of the boundary conditions using only guided modes.

The radiation from bends can be understood by considering the behavior of an equiphase wave front of a guided wave going around a bend. The fields extend outside of the rod, as shown in Figure 2-8. Much like skaters playing crack the whip, the part of the wave furthest outside the rod must increase its velocity the most to maintain the phase of the wave front. To maintain equiphase, we must have

$$hR\Delta\theta \geq k(R + x_r)\Delta\theta \tag{2-72}$$

where h is the propagation constant of a guided wave and k is the propagation constant of a wave in free space. R is the radius of curvature of the rod, and x_r is the radial distance from the center of the rod.

At the position

$$x_r = (h - k)R/k \tag{2-73}$$

the velocity of the wave front is equal to the speed of light. To make it around the curve, all of the energy in the region $x > x_r$ must propagate faster than the speed of light. This is impossible, and all of the energy in this region is radiated. Marcatili and Miller have proposed an approximate model to determine the amount of attenuation due to radiation one can expect from a bend in a slab waveguide.[17] They define a characteristic length

$$z_c = a^2/2\lambda \tag{2-74}$$

17. Marcatili, E. A. J., and Miller, S. E., "Improved Relations Describing Directional Control in Electromagnetic Wave Guidance," B.S.T.J., pp. 2161-2188, September 1969.

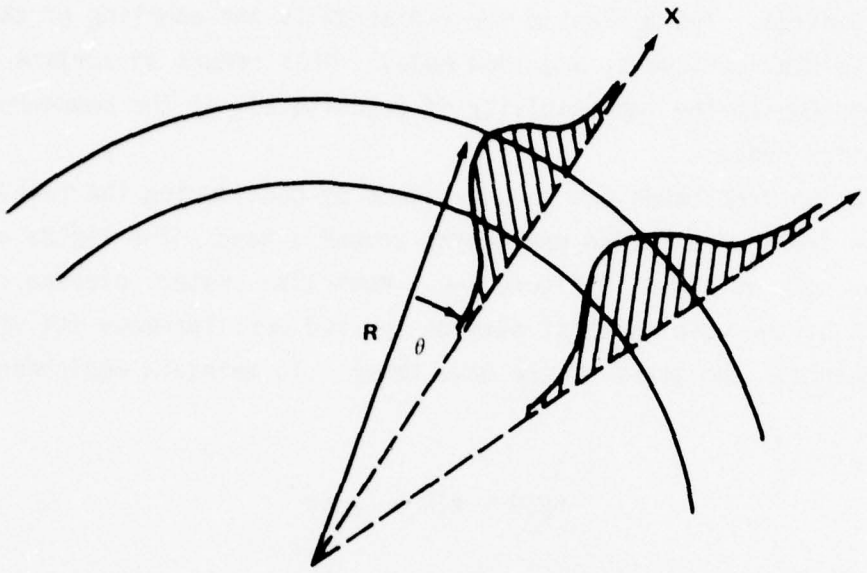

FIG. 2-8 BEND IN A DIELECTRIC WAVEGUIDE

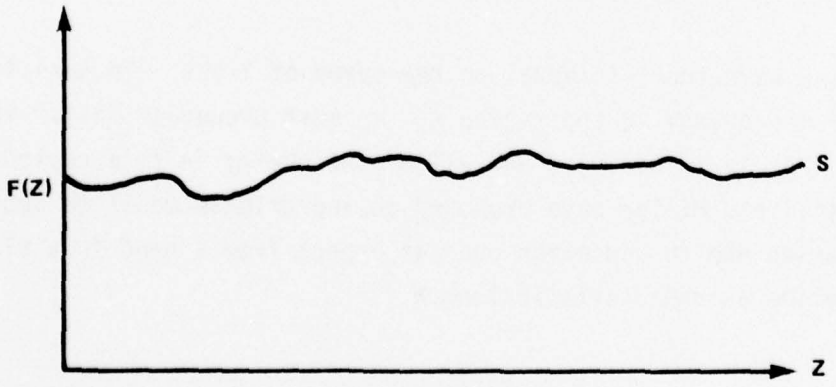

FIG. 2-9 SURFACE IMPERFECTIONS OF A SLAB WAVEGUIDE

z_c is the distance over which a beam of light will remain collimated if it has a transverse field width a and wavelength λ. They relate this to the power decay rate $\exp(-\alpha z)$, where z is the longitudinal distance along the waveguide at the bend.

The amount of energy radiated is E_L/E_T, where E_L is the amount of energy propagating at $x > x_r$, and E_T is the total energy. In a two dimensional system,

$$E_L = F^2(x)dx \tag{2-75a}$$

$$E_T = F^2(x)dz \tag{2-75b}$$

The quantity $F^2(x)$ corresponds to the energy density of the field distribution. For small α, $\exp(-\alpha z) \simeq 1 - 2\alpha z$. The fractional power loss is

$$2\alpha z_c = E_L/E_T \tag{2-76a}$$

or

$$\alpha = E_L/(2z_c E_T) \tag{2-76b}$$

It should be pointed out that this α corresponds to power attenuation due to radiation, unlike the previous section, where 2α was the power attenuation due to loss within the dielectric material.

Using this approach, it is possible to estimate the radiation loss of a rectangular dielectric waveguide using the field solutions for the unbent guide to solve for E_L and E_T. A more rigorous approach to the problem of radiation from a rectangular guide has been used to verify the validity of this approximate method.[18] However, this method is not very useful for the circular dielectric guide because of the problem of solving for E_L and E_T in a three dimensional

18. Marcatili, E. A. J., "Bends in Optical Dielectric Guides," B.S.T.J., pp. 2103-2132, September 1969.

geometry. It is also difficult to determine an appropriate value for the correlation length a. However, this approach does offer some insight into why radiation occurs.

For a large diameter rod capable of propagating more than one mode, mode coupling at a bend will often be more important than radiation. Since we are concerned only with single-mode guides, this isn't a problem.

More important than bends is the problem of radiation from surface imperfections. It's possible to make a straight dielectric guide, but there will always be some surface roughness, no matter how smooth the finish. This problem has been studied extensively, and involves the solution of coupled mode equations.[19,20,21] The theory is straightforward. One solves the boundary value problem using an infinite sum of guided and unguided modes to match boundary conditions at the irregular surface. If a single guided mode is originally propagating on the line, the degree to which it couples to other modes because of the surface imperfections can be calculated using Fourier techniques. The mathematics of this is beyond the scope of this report, but we will quote two significant results.

The surface imperfections on a dielectric guide can be described mathematically as a wall distortion function.[22] The function is just a mathematical representation of the surface profile of the guide. Consider the slab waveguide of Figure 2-9. If the height of the surface S above the z axis is f(z), and the average thickness of the slab is d, the wall distortion function is defined by

$$W = f(z) - d \qquad (2\text{-}77)$$

---

19. Snyder, A. W., "Coupling of Modes on a Tapered Dielectric Cylinder," I.E.E.E. Trans. Microwave Theory and Techniques, 18, No. 7, pp. 383-392, July 1970.
20. Collin, R. E., Field Theory of Guided Waves, McGraw-Hill, New York, 1960.
21. Marcuse, D., "Mode Conversion Caused by Surface Imperfections of a Dielectric Slab Waveguide," B.S.T.J. 48, No. 10, pp. 3177-3215, December 1969.
22. Marcuse, D., "Radiation Losses of Dielectric Waveguides in Terms of the Power Spectrum of the Wall Distortion Function," B.S.T.J. 48, No. 10, pp. 3233-3242, December 1969.

The Fourier transform of the wall distortion function is

$$\psi(\theta) = \frac{1}{L}\int_0^L [f(z) - d]e^{-i\theta z}dz \qquad (2\text{-}78)$$

where L is the length of the slab, and θ represents a spatial frequency. The spatial frequencies θ will cause radiation loss only if

$$h - k < \theta < h + k \qquad (2\text{-}79)$$

where h is the propagation constant of the mode, and k is the free space wavevector $k = \omega\sqrt{\mu_0\varepsilon_0}$.

If the Fourier transform of the wall distortion function has no spatial frequencies in this range, then there will be no radiation loss. This result is not as simple as it seems, and an interested reader is urged to consult the original literature.[22] The important conclusion, however, is that surface imperfections don't necessarily result in radiation, and that radiation may turn out not to be a problem.

Marcuse has also calculated the radiation losses from a round dielectric guide propagating the HE_{11} mode.[23] He has included the effects of random wall imperfections in terms of a correlation function. Let the power propagating on a dielectric rod be P. The power attenuation constant is related to the fractional power loss $\Delta P/P$ by

$$\alpha = (1/L)\Delta P/P \qquad (2\text{-}80)$$

where L is the length of the rod.

It is possible to find the normalized power loss as a function of the RMS deviation in the radius of the rod and a correlation length. If A is the RMS

22. Marcuse, D., "Radiation Losses of Dielectric Waveguides in Terms of the Power Spectrum of the Wall Distortion Function," B.S.T.J. 48, No. 10, pp. 3233-3242, December 1969.
23. Marcuse, D., "Radiation Losses of the Dominant Mode in Round Dielectric Waveguides," B.S.T.J., pp. 1665-1693, October 1970.

deviation in the radius a of the rod, the normalized power loss is

$$\tilde{P} = (a^3/A^2L)(\Delta P/P) \qquad (2\text{-}81)$$

Marcuse has calculated $\tilde{P}$ as a function of B/a for a teflon rod using an exponential correlation function, where B is the correlation length. This is reproduced in Figure 2-10 for several values of ka, where $k = 2\pi/\lambda_0$. The correlation length B for a given guide will generally be unknown. But the function $\tilde{P}$ turns out to be bounded from above, and it is possible to compute the worst case loss for a given value of A or vice versa.

As an example, suppose we want a teflon guide with no more than 10 dB/km radiation loss. Let the radius of the guide be 1mm, and assume the worst case value of $\tilde{P} \simeq .25$, corresponding to ka = 1.5. From equations (2-80) and (2-81), we have

$$(a^3/A^2L)\ (\Delta P/P) = (a^3\alpha)/A^2 = .25$$

$$\alpha = 10 \text{ dB/km} = 2.3 \times 10^{-3} \text{ neper/meter}$$

$$a^3 = 10^{-9} \text{ meter}$$

$$A = .003 \text{ mm}$$

Therefore, the guide radius must be uniform to within .3%. Hopefully, the value of $\tilde{P}$ will be substantially lower than worst case.

2.5 ISOLATION

Since the fields of the dielectric waveguide extend outside of the guide, they may interact with the external environment. For a practical system, this will be very important, and may pose serious problems.

One possible solution is to clad the dielectric with another dielectric material, as is done with optical fibers. The dielectric constant of the cladding is lower than that of the actual guide, but higher than the dielectric constant of free space. The field solutions inside the guide are basically unchanged, but the external fields are localized by the cladding, and are less likely to

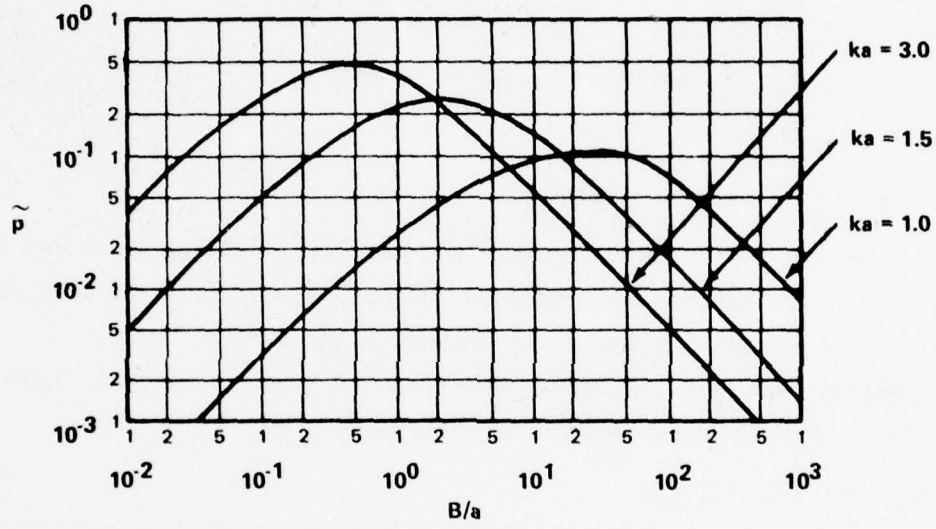

$\tilde{p} = (a^3/A^2L)\,(\Delta P/P)$

FIG. 2-10 NORMALIZED RADIATION LOSS DUE TO SURFACE IMPERFECTIONS OF A CIRCULAR DIELECTRIC GUIDE AS A FUNCTION OF CORRELATION LENGTH FOR $\epsilon = 2.05$

interact with the external surroundings. Cladding may not be the answer, however, and the specific solution to the problem will depend on the particular application for which the dielectric guide is being used.

The external field energy has been computed for the HE_{11} mode. The total stored energy within a given radius r is

$$\bar{W} = \frac{\int_0^{2\pi}\int_0^{r} \varepsilon\bar{E}\cdot\bar{E}^* + \mu_0\bar{H}\cdot\bar{H}^* \; r \, dr d\theta}{\int_0^{2\pi}\int_0^{\infty} \varepsilon\bar{E}\cdot\bar{E}^* + \mu_0\bar{H}\cdot\bar{H}^* \; r \, dr d\theta} \qquad (2\text{-}82)$$

where $\varepsilon = \varepsilon_1$ for $r \leq a$, and $\varepsilon = \varepsilon_0$ for $r > a$.

$\bar{W}$ has been computed for r = a, 2a, 5a, and 10a for polystyrene, fused quartz, and teflon. These calculations are included in the appendix, and are plotted for r = a in Figure 2-11. Note the similarity between $\bar{W}$ and R from Figure 2-7. $\bar{W}$ is the stored energy, while R relates to the Poynting power. There is approximately a factor of 2 difference between the two quantities.

2.6 POWER HANDLING CAPABILITIES

The power handling capabilities of a dielectric waveguide may depend on several different factors. Excessive power absorption may cause the material to increase in temperature and melt. Or the dielectric strength of the material can be exceeded, causing a localized breakdown. In an optical fiber, the wavelength of the light is so small that scattering is important. The power transmission is then limited by the threshold power level at which stimulated Raman and Brillouin scattering occur.

The dielectric strength of a material is typically specified at low frequencies or D.C. At microwave frequencies, the dielectric strength may be substantially different, causing the material to break down at much lower field intensities. Whether this is indeed the case for millimeter waves will be difficult to determine until high power sources become available.

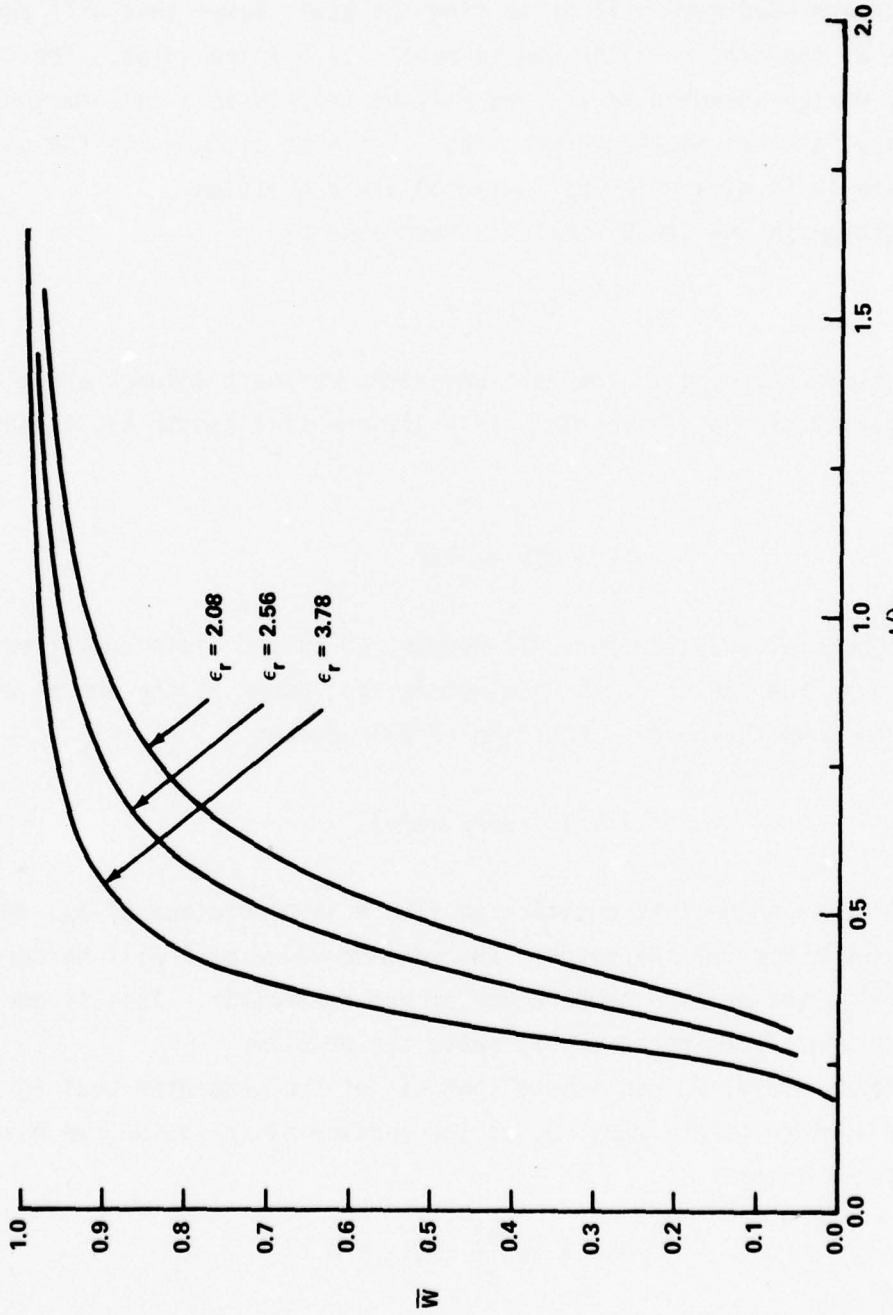

FIG. 2-11 FRACTIONAL INTERNAL ENERGY AS A FUNCTION OF d/λ_0

The problem of dielectric heating can be solved approximately to yield a rough estimate of the power that can be dissipated by a cylindrical dielectric guide. The approach used here will be to find the power level that will cause the temperature at the center of the rod to reach its melting point. The electromagnetic energy absorbed in the rod will be treated as a uniform source of heat throughout a cross-section of the rod. The heat diffuses to the outside of the rod, where it is dissipated by radiation and convection.

Heat conduction in the steady-state is described by

$$\nabla^2 T = -q/\kappa \tag{2-83}$$

where T is the temperature, q is the heat generated per unit volume, and κ is the thermal conductivity of the dielectric. In a differential length Δz, the heat generated is

$$\Delta P = q\Delta V = \alpha P \Delta z \tag{2-84}$$

where α is the power attenuation per unit length, ΔV is the differential volume element $\pi a^2 \Delta z$, a is the radius of the dielectric rod, and P is the amount of power propagating down the guide. Equation (2-83) becomes

$$\nabla^2 T = -\alpha P/(\pi a^2 \kappa) \tag{2-85}$$

We would like to solve this equation to find P as a function of T_0, the temperature at the center of the guide. The maximum value of P will be determined by setting $T_0 = T_m$, the melting temperature of the dielectric. This is one of the two boundary conditions necessary to solve the problem.

For the steady-state, we can assume that all of the generated heat is diffused to the surface of the rod. So at the surface of the guide, we have the second boundary condition,

$$q\Delta V = -\kappa \frac{\partial T}{\partial r} \Delta S \Big|_{r = a} \tag{2-86}$$

where ΔS is a unit element of surface area.

By symmetry, the θ directed component of the temperature gradient is zero. Thermal diffusion along the axis of the guide will be unimportant, so the z component can also be ignored. Equation (2-83) reduces to

$$\frac{\partial^2 T}{\partial r^2} + \frac{1}{r}\frac{\partial T}{\partial r} + \frac{\alpha P}{\pi a^2 \kappa} = 0 \qquad (2\text{-}87)$$

where $T = T_0$ at $r = 0$, and $\frac{\partial T}{\partial r} = -\alpha P/(2\pi a\kappa)$ at $r = a$.

The solution for T_0 is

$$T_0 = T_w + \alpha P/(4\pi\kappa) \qquad (2\text{-}88)$$

T_w is the surface temperature of the guide, and is determined by the ambient temperature and the effectiveness of convection and thermal radiation. The problem of finding T_w is discussed in detail by Holman, and only the results will be presented here.[24] If T_∞ is the ambient temperature outside the rod, then

$$T_0 = \frac{\alpha P}{\pi a^2}\frac{a^2}{4\kappa} + \frac{a}{2h_t} + T_\infty \qquad (2\text{-}89)$$

where h_t is an equivalent heat conduction coefficient that combines the effects of radiation and convection.

We can define h_t by

$$h_t = h_r + h_c \qquad (2\text{-}90)$$

h_r is determined by the Stefan-Boltzman law of black-body radiation, and h_c is derived using fluid mechanics.

---

24. Holman, J. P., Heat Transfer, Fourth Edition, McGraw-Hill, New York, 1976.

$$h_r \simeq \xi\sigma(T_w^2 + T_\infty^2)(T_w + T_\infty) \tag{2-91a}$$

$$h_c \simeq 1.32\{(T_w - T_\infty)/(2a)\}^{1/4} \tag{2-91b}$$

ξ is the emissivity of the dielectric, and $\sigma = 5.67 \times 10^{-8}$ Watt/m^2 °K^4.

Unfortunately, h_r, h_c, and κ are all functions of temperature. However, the dielectric rods are only a few millimeters in diameter at most, and

$$T \simeq T_0 \simeq T_w \tag{2-92}$$

As an example, consider a 2 mm teflon rod with a loss tangent of 5×10^{-4}. From the theory of section 2.3, α is found to be .0048 neper/cm. The melting point of teflon is 321°C, and the thermal conductivity is [4.86×10^{-6}T + 2.53 $\times 10^{-3}$]Watt/cm °K.[25] Depending on what value one assumes for ξ, P will be in the neighborhood of 100 to 200 Watts. Reducing the loss tangent of the material will substantially increase this amount, as will decreasing the rod diameter.

25. Brandrup and Immergut, editors, Polymer Handbook, Second Edition, Wiley & Sons, New York, 1975.

Chapter III

EXPERIMENTAL OBSERVATIONS

3.1 INTRODUCTION

Before we can legitimately use the theory of the HE_{11} mode to describe the behavior of an actual guide, it will be necessary to verify that the HE_{11} mode actually propagates when a wave is launched on a dielectric rod. From Chapter 2, we know that for a given d/λ_0 and ε, the HE_{11} mode will be characterized by a certain λ/λ_0. If we assume that the HE_{11} mode is propagating, then measurement of d/λ_0 and λ/λ_0 will yield a value for ε. If this ε agrees with the known ε for the material, we can be sure that the HE_{11} mode is propagating. We can look for the presence of other modes by probing the standing wave pattern on the rod. Since each mode has its own characteristic wavelength, the presence of more than one mode will be readily apparent. This method has been used by Cullen and Gillespie to study the properties of a glass rod at 33 GHz.[26]

Unfortunately, values for ε at 70 GHz are not available for most materials. However, dielectric constant varies slowly with frequency, and we can approximate ε with a value measured at a lower frequency (i.e., 25 GHz). The difference in λ/λ_0 between each of the lowest order modes is substantial enough that only approximate agreement between the observed and known values for ε is necessary to confirm the presence of the HE_{11} mode. Once this is verified, we can assume that the observed value of ε is the actual dielectric constant of the material at 70 GHz. Thus measurement of d/λ_0 and λ/λ_0 will yield a previously unknown value for ε at 70 GHz, as well as verify the presence of the dipole mode.

The attenuation characteristics of the dielectric rod are of critical importance in determining the practicality of using the rod as a waveguide. In Chapter 2, it was seen that knowledge of the loss tangent of the dielectric will

26. Cullen, A. L., and Gillespie, E. F. F., "A New Method for Dielectric Measurements at Millimeter Wavelengths," Presented at the Symposium on Millimeter Waves, Polytechnic Institute of Brooklyn, April 1959.

yield an attenuation factor for the guide. However, this does not include the attenuation due to radiation, which may be significant. In most cases, data for tan δ at 70 GHz isn't available. Thus it is desirable to measure the attenuation directly. We can relate this measured attenuation to an equivalent tan δ' that will include the effects of radiation. In those cases where the intrinsic loss tangent of the material is known, comparison of tan δ with tan δ' will allow one to determine how much energy is lost to radiation.

The method used to determine the guide wavelength and attenuation factor is relatively simple. A klystron is used to excite the HE_{11} mode on a long section of dielectric rod. A probe that can move up and down the length of the rod on a motorized cart is attached. The movement of the probe is synchronized with a chart recorder so that one can plot the average power propagating on the rod as a function of position. The power decays exponentially as the probe moves down the line, thus yielding the attenuation factor. If a metal reflector is attached to the end of the dielectric rod, a standing wave is set up and the guide wavelength can also be determined.

Figure (3-1) shows the apparatus used. The dielectric rod is butted against the metal waveguide and is held in place by four set screws. The other end of the rod is pulled taught and held with a clamp. For the first experiments, the probe consisted of a short piece of dielectric rod butted into a metal waveguide containing a diode detector. This dielectric probe is placed in proximity to the rod being measured. In later measurements, the probe was a piece of metal waveguide with a hold drilled through the top. The dielectric waveguide passes through the hole, thus coupling the longitudinal E field of the HE_{11} mode to the TE_{10} mode of the rectangular guide. Other probe configurations were tried, but this was the most successful.

It is essential that the dielectric rod being measured be as long as possible. If the dielectric rod is too short, the attenuation may be too little to measure accurately. In addition, the VSWR caused by a reflection at the end of the rod will increase significantly and make the attenuation seem lower than it really is. (The probe will detect the sum of the incident and reflected waves; this sum does not decay exponentially, as examination of basic transmission line theory will show. If the rod is sufficiently long, the initial wave will decay enough so that a reflection at the end of the rod will be insignificant).

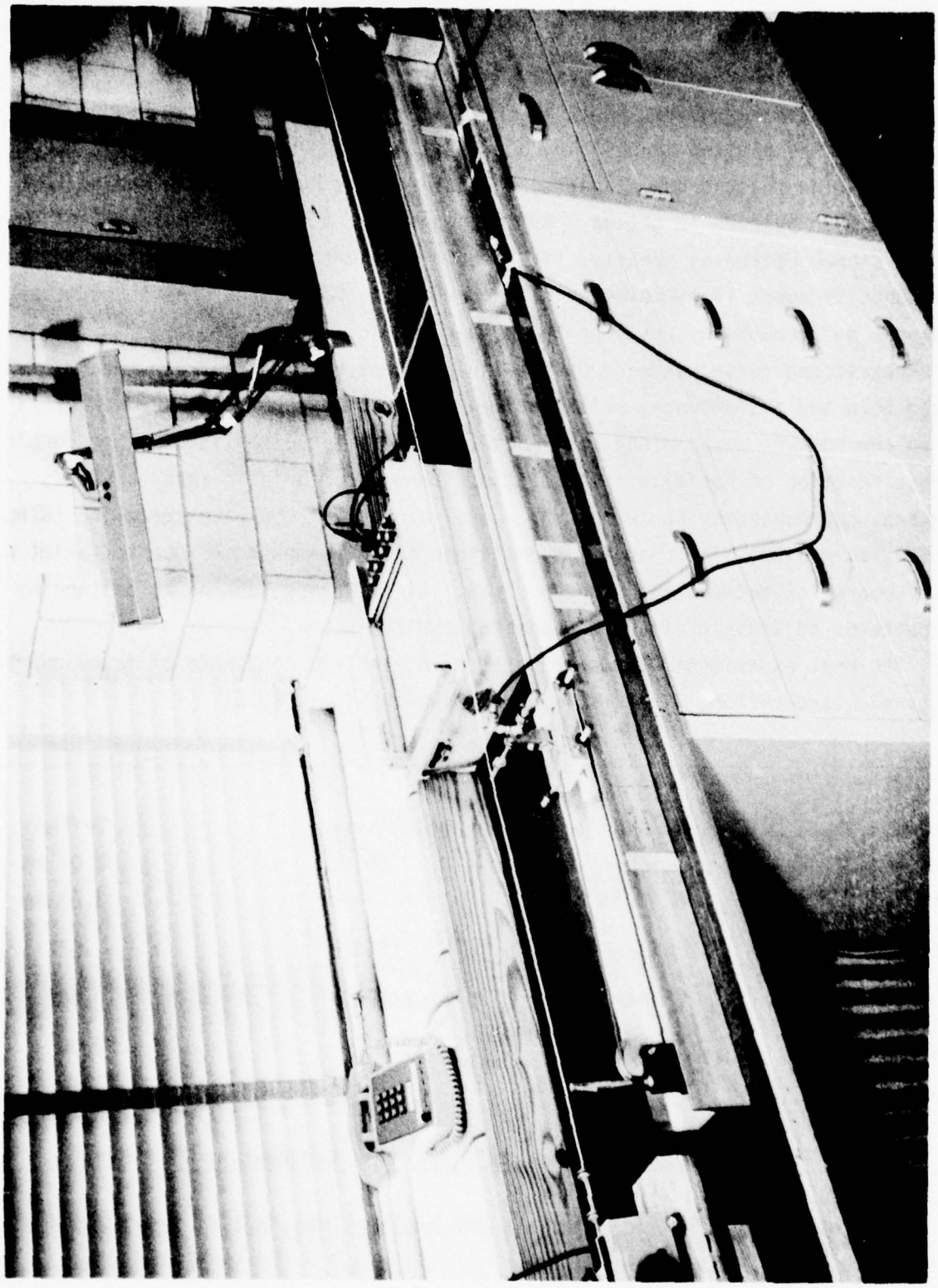

Fig. 3-1 Experimental Apparatus

3.2 EXPERIMENTAL RESULTS

The very first experiment was to determine that the dielectric rod was indeed acting as a waveguide. This is the case, as can be seen from Figure 3-2. The top curve was plotted by pointing a transmitting and receiving horn at each other and moving the two horns apart. The gain of the horns is high enough that a standing wave pattern is set up. As the horns move apart, the amplitude of the received signal decreases greatly. The length of the top curve in the figure corresponds to about 15 cm movement of the receiving horn, The free space wavelength can be computed by counting the number of oscillations.

The second curve was made by placing a polystyrene rod between the transmitting horn and a stationary reflector. A dielectric probe was placed in proximity to the rod and moved along its length. Note that the amplitude is no longer a strong function of position. In addition, the characteristic wavelength has decreased, corresponding to the slower phase velocity of the wave traveling through a dielectric medium. The changes in amplitude along the path are due to variation in the separation between the probe and rod. Since we are looking at a standing wave pattern, adjacent minima are separated by $\lambda/2$, not λ.

The next experiment was to measure the dielectric constants of fused quartz, polystyrene, and teflon. The results are shown in Figure (3-3).

MATERIAL	Fused Quartz	Polystyrene	Teflon
Rod diam.	1.09 mm	2.38 mm	2.01 mm
d_c	1.95 mm	2.62 mm	3.24 mm
d/λ_0	.259	.563	.477
λ/λ_0	.980	.811	.947
ε	3.75	2.53	2.00
ε(25 GHz)[28]	3.78	2.56	2.08

Figure 3-3 Measurement of Dielectric Constant at 71.0 GHz

28. VonHippel, A., Dielectric Materials and Applications, M.I.T. Press and John Wiley & Sons, New York, 1954.

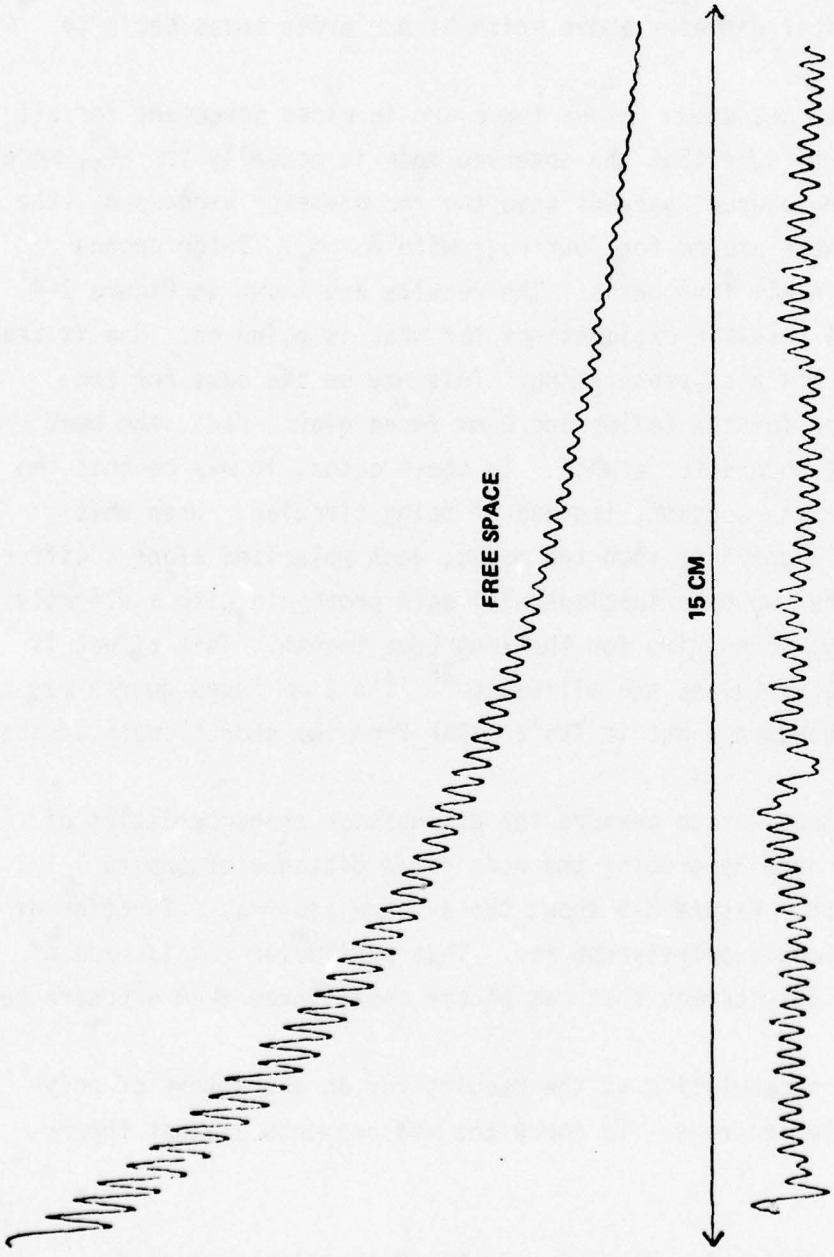

FIG. 3-2 STANDING WAVE PATTERN OF A ROUND DIELECTRIC GUIDE

The guide wavelength was measured by probing a section of dielectric rod. λ_0 was determined by measuring the frequency of the klystron with a cavity wavemeter. The rod diameter was measured with a micrometer. ε is computed using a Fortran program to find a best fit to the guidance condition of the HE_{11} mode. The quantity d_c corresponds to the critical diameter above which higher order modes begin to propagate.

Since the measured and known values for ε are in close agreement for all three materials, we can be sure that the observed mode is actually the HE_{11} mode.

To see if anything unusual happens when the rod diameter exceeds d_c, the standing wave patterns were probed for four rods with $d > d_c$. Interference patterns were observed in all four cases. The results are shown in Figure 3-4.

There are several possible explanations for what is going on. One is that the TE_{01} and TM_{01} modes are also propagating. This may be the case for the 3.24 mm polystyrene. But for the teflon and 2 mm fused quartz rods, the beat length is too long to be mode interference. In these cases, it may be that the rods are elliptical in cross-section, instead of being circular. When this happens, the HE_{11} mode is split up into two modes, each polarized along a different axis of the ellipse. The two polarizations will each propagate with a slightly different phase velocity, accounting for the long beat length. This effect is discussed in more detail by Cullen and Gillespie.[26] The 3 mm fused quartz may be experiencing the same phenomena, but it isn't clear from the short length of the plot.

The final experiment was to measure the attenuation characteristics of various rods. This was done by probing the rods for a distance of one to 1 1/2 meters along their length. Figure 3-5 shows the average power as a function of length for 1.5 meters along a polystyrene rod. This particular rod is made of Rexolite 1422, which is polystyrene that has become crosslinked from exposure to radiation.

Figure 3-6 shows a tabulation of the results for an assortment of polystyrene, Rexolite, and teflon rods. To check the measurements against theory,

---

26. Cullen, A. L., and Gillespie, E. F. F., "A New Method for Dielectric Measurements at Millimeter Wavelengths," Presented at the Symposium on Millimeter Waves," Polytechnic Institute of Brooklyn, April 1959.

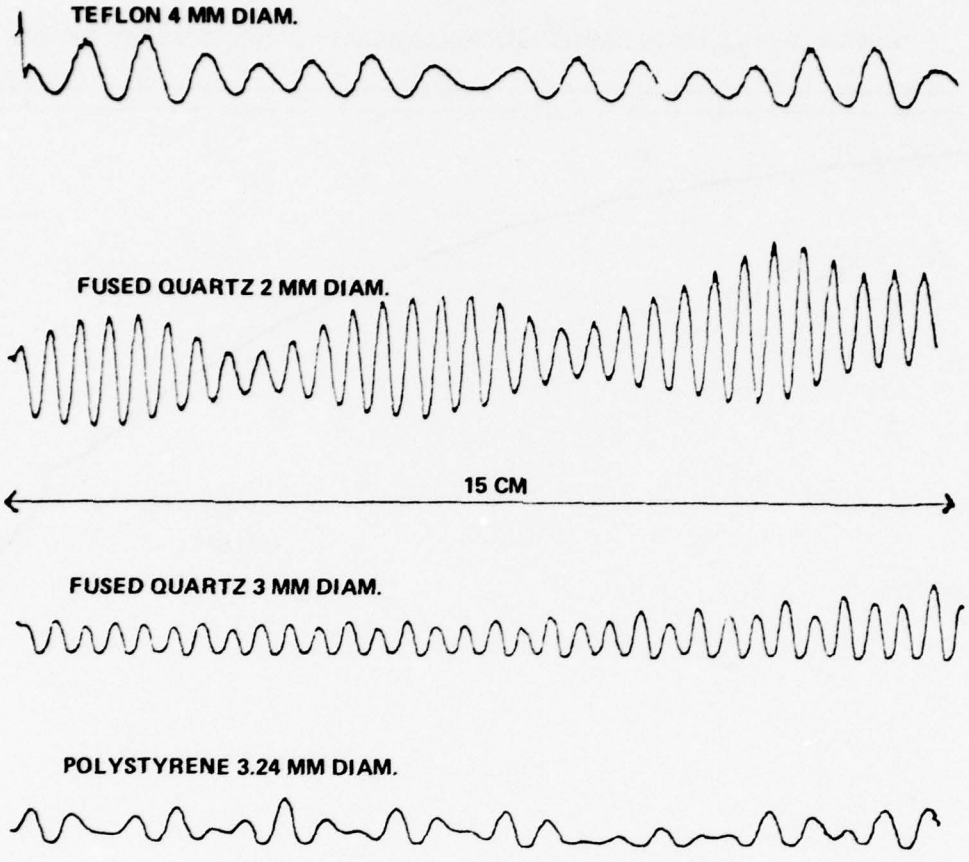

FIG. 3-4 INTERFERENCE PATTERNS OF A DIELECTRIC ROD

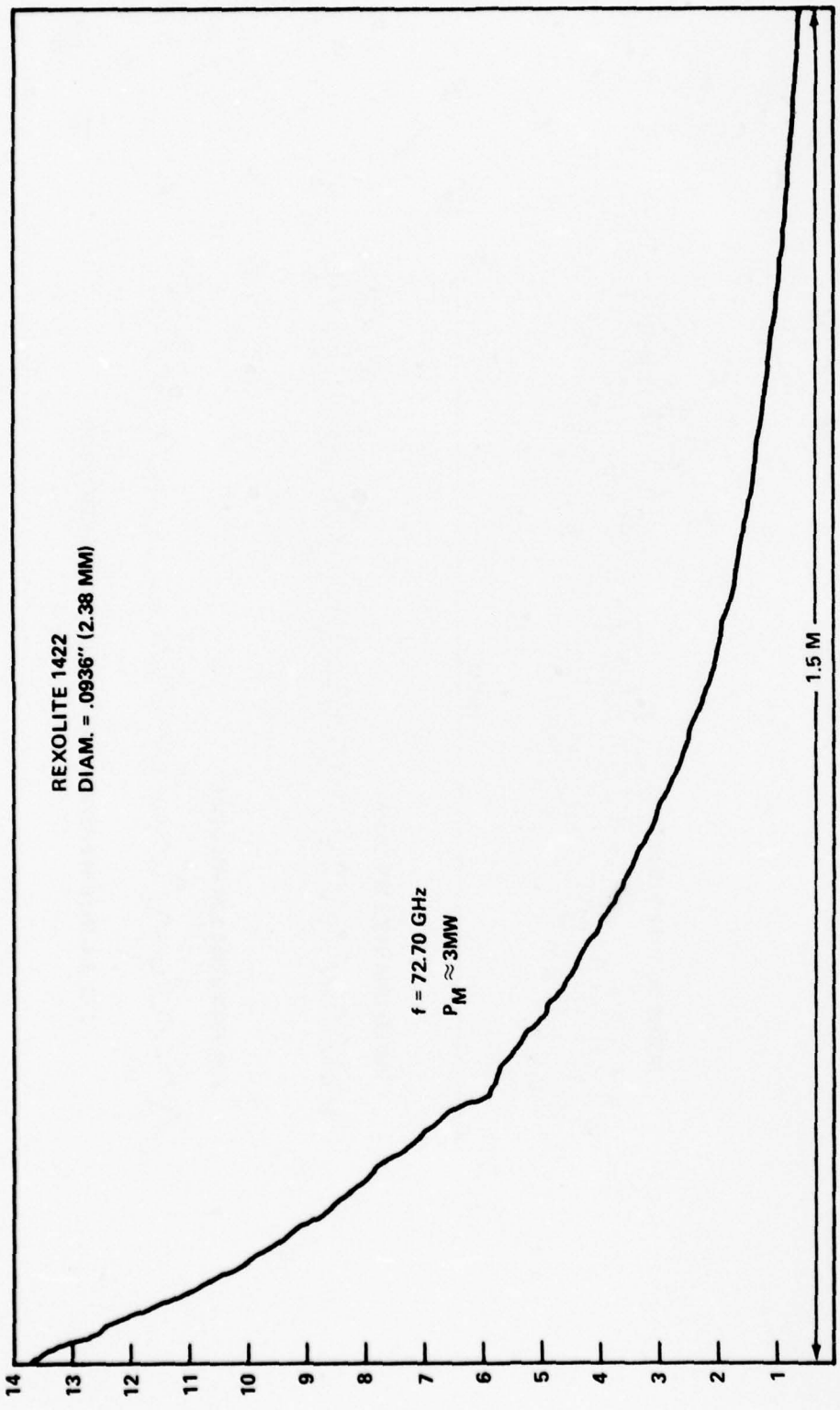

FIG. 3-5 AVERAGE POWER AS A FUNCTION OF LENGTH FOR A DIELECTRIC ROD

MATERIAL	DIAMETER (mm)	d/λ_0	POWER ATTENUATION (dB/meter)	R	tan δ
Rexolite	1.60	.3877	3.93	.2251	.00103
"	2.38	.5768	9.06	.5439	.00098
"	3.20	.7755	10.10	.6233	.00096
Polystyrene	3.32	.8045	11.25	.6288	.00106
"	3.63	.8797	12.47	.6350	.00116
Teflon	2.01	.4871	.83	--	--
"	3.00	.7270	1.90	--	--

Figure (3-6) ATTENUATION FACTORS OF VARIOUS DIELECTRIC WAVEGUIDES AT 72.70 GHz

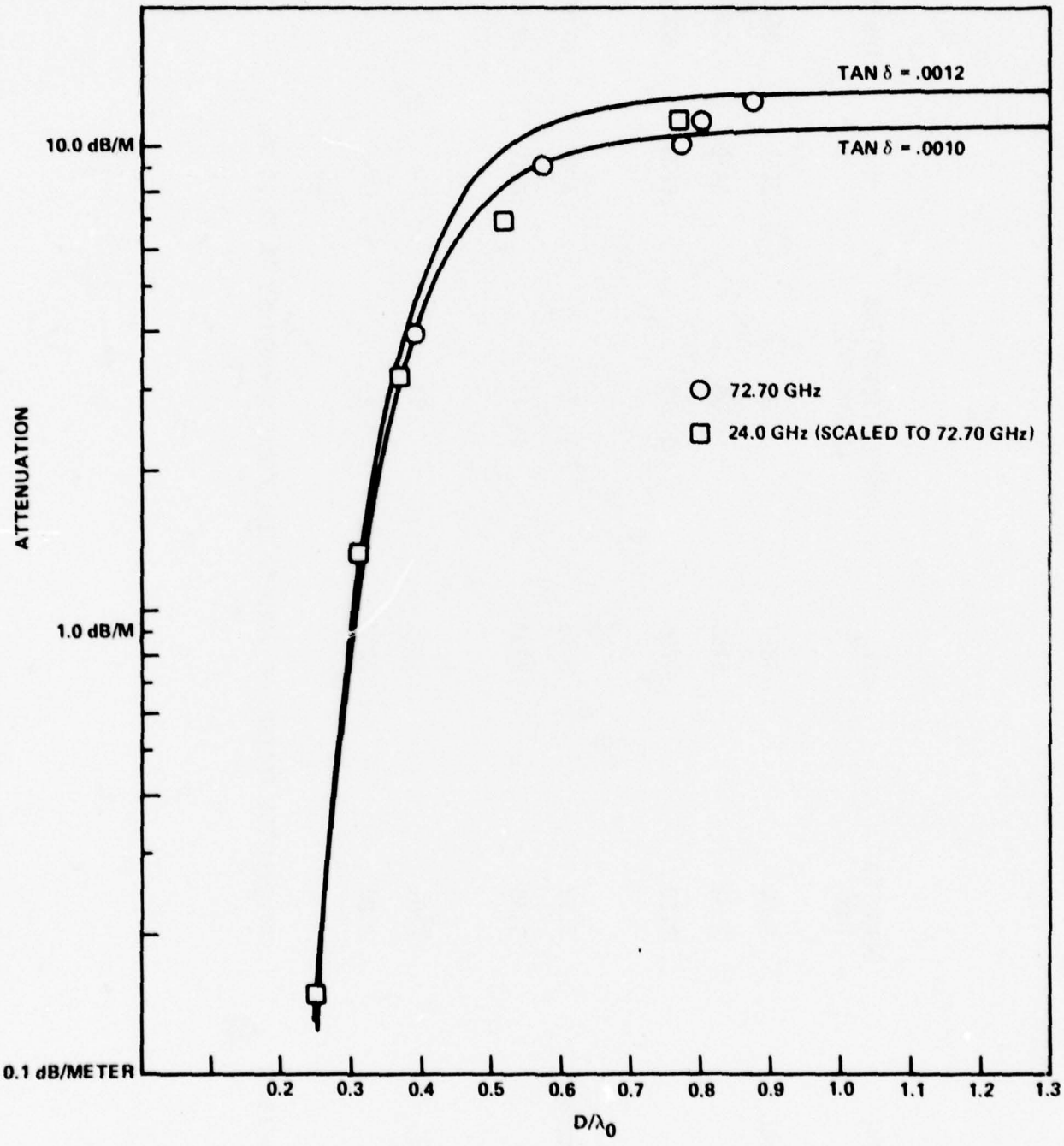

FIG. 3-7 ATTENUATION AS A FUNCTION OF DIAMETER FOR ϵ = 2.56

the loss tangent is computed for the various polystyrene and Rexolite rods. This was not very difficult, as the numerical calculations for attenuation as a function of rod diameter have already been done by Elsasser[16] for $\varepsilon = 2.56$ (see section 2.3). The results are plotted in Figure 3-7. The solid lines represent the theoretical calculations for various values of tan δ. The experimental data also includes measurements made at 24 GHz by Chandler.[27]

Some of the larger rods exceed the critical diameter, and more than one mode may be propagating. Since the attenuation of each mode is slightly different, the experimental data for these rods may not represent the true attenuation of the HE_{11} mode. However, the results for the larger rods are consistent enough to warrant their inclusion.

The computer values of tan δ appear to be self consistent, thus supporting the validity of Elsasser's theory. However, there is no independent data for tan δ of polystyrene at 70 GHz with which to compare these results. There is a possibility that some of the attenuation is due to radiation, and that the measured tan δ' is higher than the intrinsic tan δ of the material. Measurements of tan δ have been made for polystyrene and Rexolite at 25 GHz,[28] and for polystyrene at 400 GHz.[29] Although the data reported in Von Hippel varies substantially from sample to sample, it is clear that tan δ rises dramatically between 24 and 400 GHz. At 24 GHz, tan δ is roughly 5×10^{-4}; at 400 GHz, tan δ is reported as 6×10^{-3}. Our experimental data indicates that tan δ is approximately 10^{-3} at 72.70 GHz. The indications are that radiation loss is not significant.

The overall conclusion to be drawn is that dielectric waveguide can be designed to have lower loss than metal waveguide at these frequencies, simply by decreasing the diameter. The polystyrene has substantially more loss than the

---

16. Elsasser, W. M., "Attenuation in a Dielectric Circular Rod," J. Appl. Phys. 20, p. 1193, December 1949.
27. Chandler, C. H., "An Investigation of Dielectric Rod as Wave Guide," Journal of Applied Physics, 20, p. 1188, December 1949.
28. VonHippel, A., Dielectric Materials and Applications, M.I.T. Press and John Wiley & Sons, New York, 1954.
29. Breeden, K. H., and Sheppard, A. P., "A Note on the Millimeter and Submillimeter Wave Dielectric Constant and Loss Tangent Value of Some Common Materials," Radio Science, Vol. 3, No. 2., February 1968.

teflon, primarily for two reasons. The teflon has a slightly lower dielectric constant, resulting in less energy propagating within the rod for a given diameter. In addition, teflon is a nonpolar polymer. This makes it relatively inert in the presence of an external field. Polystyrene, on the other hand, is extremely polar. This results in a strong interaction between the individual molecules and the applied electric field, which in turn causes loss.[30]

30. P. Debye, Polar Molecules, Dover Publications, New York, NY, 1945.

Chapter IV

SUMMARY AND CONCLUSIONS

In this report, we have approached the subject of the dielectric waveguide from both a theoretical and experimental point of view. Even though the discussion has been limited to the dominant mode of the cylindrical guide, the theory is complicated and the mathematics difficult. Although they seem straightforward, the experimental techniques involve a great deal of numerical analysis, and require a thorough understanding of basic theory.

Our discussion provides a qualitative understanding of the basic behavior of a dielectric waveguide. The experiments have confirmed that the basic theory is sound, and that the use of dielectric rods for making millimeter wave transmission lines is not unreasonable.

To summarize briefly, the behavior of a dielectric waveguide is determined by the electrical and magnetic properties of the material, and by the physical structure of the waveguide. For a homogeneous, non-magnetic material, the major difficulty lies in the solution of Maxwell's equations subject to the appropriate boundary conditions. The most important property of any dielectric waveguide is that the field solutions can be separated into a discrete set of guided modes, and a continuous set of radiation modes. Each guided mode is characterized by an eigenvalue h and a phase velocity ω/k. The guided modes decay at large distances from the guide and do not radiate energy. However, a substantial portion of the energy of the guided mode propagates outside of the guide.

The attenuation factor of the guide depends on the loss tangent of the dielectric material, and on the extent to which the energy of the mode is contained within the dielectric. By reducing the guide dimensions, the relative amount of energy propagating outside of the guide is increased, and the attenuation factor is decreased. The limiting factor in reducing the attenuation is the critical guide cross section below which a given mode is cutoff and doesn't

propagate. The dominant mode of the circular guide has no cutoff, and in principle, the attenuation of this mode can be made arbitrarily small.

Radiation loss is caused by the coupling between guided and radiation modes. This occurs at bends in the guide or at surface imperfections. A perfectly straight guide with no surface imperfections will not radiate. If the spatial frequencies of the Fourier transform of the surface profile of the guide are not in a given frequency range, then radiation due to surface imperfections will be minimal. Radiation at bends is due to the impossibility of a wave front propagating around a bend at a speed greater than the speed of light. For large diameter guides, mode coupling will often be more important than radiation.

The amount of power absorbed by a dielectric guide depends on the loss tangent, the homogeneity of the material, and the field distributions inside the guide. The ability of the guide to dissipate energy will depend on the size and shape of the guide, the thermal conductivity of the dielectric, and the effectiveness of convection and thermal radiation at the surface of the guide. For the steady state, one can approximate the maximum amount of energy that can be dissipated by a guide without its melting. However, inhomogeneities in the dielectric will probably cause localized breakdown of the rod at much lower power levels, so that this analysis is only approximate.

In this study, we have experimentally determined the dielectric constants of samples of fused quartz, polystyrene, and teflon at a frequency of 71.0 GHz. The results are consistent with values of ε_r measured at other frequencies. The attenuation factor was measured for various dielectric rods at 71.7 GHz. The attenuation factors for polystyrene were related to an equivalent loss tangent for the material that includes the effects of both radiation and absorption loss. Comparison of this result with other data indicates that radiation loss probably is not significant.

There is a major problem that has only been touched on in this report. The manufacturing techniques have a very large effect on the electrical properties of a material, and there is often a large disparity between the electrical properties of various samples of the same material. Unless the chemical and mechanical properties of a dielectric sample are also specified, it is not accurate to say that the measured electrical properties represent the true properties of anything except the particular sample used in the experiment. For example, the degree of

crystallinity of a teflon rod may be different than that of a teflon slab, because of the different manufacturing processes involved. Consequently, the complex dielectric constant of a teflon slab will be slightly different than that of a teflon rod. The amount of impurities will have a major effect on the electrical properties. But the amount of impurities also varies strongly between samples.

Unless a material is specifically designed for electrical applications, it is unlikely that it will be very pure. For instance, plasticizers are routinely added to many polymers (i.e. - polystyrene) to improve their mechanical properties. The addition of a plasticizer will change the dielectric constant and raise the loss tangent.

The materials used in the experiments were not designed with millimeter wave applications in mind, and there is no doubt that their properties at millimeter wave frequencies can be improved. In addition to decreasing the amount of impurities in the materials, techniques such as cross-linking the polymers or casting the materials in a vacuum instead of air will substantially improve the dielectric and attenuation characteristics of the materials.

The effect of temperature on dielectric properties is also a major problem that will have to be solved.

The point is that the development and understanding of materials is a critical issue in the design of practical dielectric devices. This is true for any structure be it dielectric waveguide, stripline, microstrip, or whatever.

In this report, we have shown that a dielectric rod waveguide can guide a wave with an amount of attenuation that is lower than that of a rectangular metal guide. The dielectric waveguide has poor isolation, and is difficult to interface with other structures. But it is extremely inexpensive compared to other structures, and is simple from a physical point of view.

Further work needs to be done in several areas. The theory needs to be extended to higher order modes and to topologies other than the circular rod. The measurement techniques must be improved until they are simple, accurate, and versatile enough for general use in analyzing materials. The study of materials is of critical importance, as the practicality of any structure will be determined by the material's properties. And finally, the design of components such as antennas, phase shifters, delay lines, and couplers, is a wide open area.

Dielectric waveguide may not be the ultimate waveguiding structure, but there is no doubt that it will be useful for some applications, particularly antennas and long distance transmission lines. Ten years ago, few people would have believed that optical fibers would be practical for telephone communications. But the widespread use of such fibers is just around the corner. Ten years from now, the use of dielectric waveguide at millimeter wave frequencies may be just as practical.

REFERENCES

1. Abele, T. A. et al., "A High-Capacity Digital Communication System Using TE_{01} Transmission in Circular Waveguide," IEEE Trans. Microwave Theory & Tech., Vol. MTT-23, pp. 326-333, April 1975.

2. Hondros and Debye, "Electromagnetische Wellen an dielektrischen Drahten," Ann. der Phys., Vol. 32, pp. 465-476, June 1910.

3. Cullen, A. L., and Gillespie, E. F. F., "A New Method for Dielectric Measurements at Millimeter Wavelengths," Presented at the Symposium on Millimeter Waves, Polytechnic Institute of Brooklyn, April 1959.

4. TIME Magazine, Science Section, March 22, 1976.

5. Elsasser, W. M., "Attenuation in a Dielectric Circular Rod," J. Appl. Phys. 20, p. 1193, December 1949.

6. Marcatili, E. A. J., "Bends in Optical Dielectric Guides," Bell System Technical Journal, pp. 2103-2132, September 1969.

7. Marcuse, D., and Derosier, R.M., "Mode Conversion Caused by Diameter Changes of a Round Dielectric Waveguide," B.S.T.J. 48, No. 10, pp. 3217-3232, December 1969.

8. Marcuse, D., "Radiation Losses of the Dominant Mode in Round Dielectric Waveguides," B.S.T.J., pp. 1665-1693, October 1970.

9. Marcuse, D., "Radiation Losses of Dielectric Waveguides in Terms of the Power Spectrum of the Wall Distortion Function," B.S.T.J., pp. 3233-3242, December 1969.

10. Stratton, J. A., Electromagnetic Theory, McGraw-Hill, New York, 1941.

11. Marcuse, D., "Mode Conversion Caused by Surface Imperfections of a Dielectric Slab Waveguide," B.S.T.J. 48, No. 10, pp. 3177-3215, December 1969.

12. Kapany, N.S., and Burke, J.J., Optical Waveguides, Academic Press, New York, 1972, p. 96.

13. Ibid, p. 118.

14. Ibid, p. 150.

15. Marcuse, D., "Radiation Losses of the Dominant Mode in Round Dielectric Waveguides," B.S.T.J., pp. 1665-1693, October 1970.

16. Elsasser, W. M., "Attenuation in a Dielectric Circular Rod," J. Appl. Phys. 20, p. 1193, December 1949.

REFERENCES (Cont.)

17. Marcatili, E. A. J., and Miller, S. E., "Improved Relations Describing Directional Control in Electromagnetic Wave Guidance," B.S.T.J., pp. 2161-2188, September 1969.

18. Marcatili, E. A. J., "Bends in Optical Dielectric Guides," B.S.T.J., pp. 2103-2132, September 1969.

19. Snyder, A. W., "Coupling of Modes on a Tapered Dielectric Cylinder," I.E.E.E. Trans. Microwave Theory and Techniques, 18, No. 7, pp. 383-392, July 1970.

20. Collin, R. E., Field Theory of Guided Waves, McGraw-Hill, New York, 1960.

21. Marcuse, D., "Mode Conversion Caused by Surface Imperfections of a Dielectric Slab Waveguide," B.S.T.J. 48, No. 10, pp. 3177-3215, December 1969.

22. Marcuse, D., "Radiation Losses of Dielectric Waveguides in Terms of the Power Spectrum of the Wall Distortion Function," B.S.T.J. 48, No. 10, pp. 3233-3242, December 1969.

23. Marcuse, D., "Radiation Losses of the Dominant Mode in Round Dielectric Waveguides," B.S.T.J., pp. 1665-1693, October 1970.

24. Holman, J. P., Heat Transfer, Fourth Edition, McGraw-Hill, New York, 1976.

25. Brandrup and Immergut, editors, Polymer Handbook, Second Edition, Wiley & Sons, New York, 1975.

26. Cullen, A. L., and Gillespie, E. F. F., "A New Method for Dielectric Measurements at Millimeter Wavelengths," Presented at the Symposium on Millimeter Waves, Polytechnic Institute of Brooklyn, April 1959.

27. Chandler, C. H., "An Investigation of Dielectric Rod as Wave Guide," Journal of Applied Physics, 20, p. 1188, December 1949.

28. VonHippel, A., Dielectric Materials and Applications, M.I.T. Press and John Wiley & Sons, New York, 1954.

29. Breeden, K. H., and Sheppard, A. P., "A Note on the Millimeter and Submillimeter Wave Dielectric Constant and Loss Tangent Value of Some Common Materials," Radio Science, Vol. 3, No. 2., February 1968.

30. P. Debye, Polar Molecules, Dover Publications, New York, NY, 1945.

Appendix A

NUMERICAL COMPUTATIONS

Solutions to the guidance condition of the HE_{11} mode have been calculated for values of ε corresponding to teflon (2.08), polystyrene (2.56), and fused quartz (3.78). The data is tabulated on the following pages.

The diameter factor refers to the distance from the rod within which the fractional internal energy was computed. The calculation of the fractional internal energy is discussed in chapter 2.

Z1 and Z2 are calculation parameters that are related to the Hankel and Bessel functions that describe the electric and magnetic fields.

PERMITTIVITY = 2.08

DIAMETER FACTOR = 1.00

Z1.	Z2	LAMBDA G / LAMBDA 0	DIAMETER / LAMBDA 0	FRACTIONAL INTERNAL ENERGY	FRACTIONAL EXTERNAL ENERGY
1.0000	.0797	.9966	.3073	.0580	.9420
1.0500	.1082	.9944	.3233	.0869	.9131
1.1000	.1421	.9913	.3397	.1223	.8777
1.1500	.1816	.9871	.3566	.1637	.8363
1.2000	.2270	.9818	.3741	.2101	.7899
1.2500	.2790	.9753	.3923	.2606	.7394
1.3000	.3379	.9675	.4114	.3143	.6857
1.3500	.4045	.9583	.4317	.3700	.6300
1.4000	.4798	.9477	.4533	.4268	.5732
1.4500	.5648	.9356	.4766	.4838	.5162
1.5000	.6610	.9223	.5021	.5403	.4597
1.5500	.7702	.9076	.5301	.5955	.4045
1.6000	.8946	.8919	.5615	.6487	.3513
1.6500	1.0372	.8751	.5969	.6993	.3007
1.7000	1.2016	.8575	.6376	.7467	.2533
1.7500	1.3930	.8395	.6851	.7906	.2094
1.8000	1.6177	.8213	.7413	.8306	.1694
1.8500	1.8846	.8032	.8089	.8662	.1338
1.9000	2.2064	.7856	.8919	.8974	.1026
1.9500	2.6001	.7690	.9955	.9239	.0761
2.0000	3.0908	.7535	1.1276	.9457	.0543
2.0500	3.7207	.7395	1.3012	.9633	.0367
2.1000	4.5557	.7273	1.5365	.9767	.0233
2.1500	5.7202	.7168	1.8717	.9864	.0136
2.2000	7.4414	.7083	2.3768	.9930	.0070
2.2500	10.2832	.7017	3.2242	.9970	.0030

PERMITTIVITY = 2.08

DIAMETER FACTOR = 2.00

Z1	Z2	LAMBDA G / LAMBDA 0	DIAMETER / LAMBDA 0	FRACTIONAL INTERNAL ENERGY	FRACTIONAL EXTERNAL ENERGY
1.0000	.0797	.9966	.3073	.1593	.8407
1.0500	.1082	.9944	.3233	.2280	.7720
1.1000	.1421	.9913	.3397	.3060	.6940
1.1500	.1816	.9871	.3566	.3896	.6104
1.2000	.2270	.9818	.3741	.4750	.5250
1.2500	.2790	.9753	.3923	.5588	.4412
1.3000	.3379	.9675	.4114	.6380	.3620
1.3500	.4045	.9583	.4317	.7105	.2895
1.4000	.4798	.9477	.4533	.7747	.2253
1.4500	.5648	.9356	.4766	.8298	.1702
1.5000	.6610	.9223	.5021	.8757	.1243
1.5500	.7702	.9076	.5301	.9125	.0875
1.6000	.8946	.8919	.5615	.9411	.0589
1.6500	1.0372	.8751	.5969	.9622	.0378
1.7000	1.2016	.8575	.6376	.9772	.0228
1.7500	1.3930	.8395	.6851	.9872	.0128
1.8000	1.6177	.8213	.7413	.9934	.0066
1.8500	1.8846	.8032	.8089	.9969	.0031
1.9000	2.2064	.7856	.8919	.9988	.0012
1.9500	2.6001	.7690	.9955	.9996	.0004
2.0000	3.0908	.7535	1.1276	.9999	.0001
2.0500	3.7207	.7395	1.3012	1.0000	.0000
2.1000	4.5557	.7273	1.5365	1.0000	.0000
2.1500	5.7202	.7169	1.8717	1.0000	.0000
2.2000	7.4414	.7083	2.3768	1.0000	.0000
2.2500	10.2932	.7017	3.2242	1.0001	-.0001

PERMITTIVITY = 2.08

DIAMETER FACTOR = 5.00

Z1	Z2	LAMBDA G / LAMBDA 0	DIAMETER / LAMBDA 0	FRACTIONAL INTERNAL ENERGY	FRACTIONAL EXTERNAL ENERGY
1.0000	.0797	.9966	.3073	.4357	.5643
1.0500	.1082	.9944	.3233	.5630	.4370
1.1000	.1421	.9913	.3397	.6800	.3200
1.1500	.1816	.9871	.3566	.7789	.2211
1.2000	.2270	.9818	.3741	.8560	.1440
1.2500	.2790	.9753	.3923	.9120	.0880
1.3000	.3379	.9675	.4114	.9496	.0504
1.3500	.4045	.9583	.4317	.9732	.0268
1.4000	.4798	.9477	.4533	.9868	.0132
1.4500	.5648	.9356	.4766	.9941	.0059
1.5000	.6610	.9223	.5021	.9976	.0024
1.5500	.7702	.9076	.5301	.9991	.0009
1.6000	.8946	.8919	.5615	.9997	.0003
1.6500	1.0372	.8751	.5969	.9999	.0001
1.7000	1.2016	.8575	.6376	1.0000	.0000
1.7500	1.3930	.8395	.6851	1.0000	.0000
1.8000	1.6177	.8213	.7413	1.0000	.0000
1.8500	1.8846	.8032	.8089	1.0000	.0000
1.9000	2.2064	.7856	.8919	1.0000	.0000
1.9500	2.6001	.7690	.9955	1.0000	.0000
2.0000	3.0908	.7535	1.1276	1.0000	-.0000
2.0500	3.7207	.7395	1.3012	1.0000	.0000
2.1000	4.5557	.7273	1.5365	1.0000	-.0000
2.1500	5.7202	.7168	1.8717	1.0064	-.0064
2.2000	7.4414	.7083	2.3768	******	******
2.2500	10.2832	.7017	3.2242	R	-R

PERMITTIVITY = 2.08

DIAMETER FACTOR =10.00

Z1	Z2	LAMBDA G / LAMBDA 0	DIAMETER / LAMBDA 0	FRACTIONAL INTERNAL ENERGY	FRACTIONAL EXTERNAL ENERGY
1.0000	.0797	.9966	.3073	.7293	.2707
1.0500	.1082	.9944	.3233	.8429	.1571
1.1000	.1421	.9913	.3397	.9184	.0816
1.1500	.1816	.9871	.3566	.9622	.0378
1.2000	.2270	.9818	.3741	.9845	.0155
1.2500	.2790	.9753	.3923	.9944	.0056
1.3000	.3379	.9675	.4114	.9982	.0018
1.3500	.4045	.9583	.4317	.9995	.0005
1.4000	.4798	.9477	.4533	.9999	.0001
1.4500	.5648	.9356	.4766	1.0000	.0000
1.5000	.6610	.9223	.5021	1.0000	.0000
1.5500	.7702	.9076	.5301	1.0000	.0000
1.6000	.8946	.8919	.5615	1.0000	.0000
1.6500	1.0372	.8751	.5969	1.0000	.0000
1.7000	1.2016	.8575	.6376	1.0000	.0000
1.7500	1.3930	.8395	.6851	1.0000	.0000
1.8000	1.6177	.8213	.7413	1.0000	-.0000
1.8500	1.8846	.8032	.8089	1.0000	-.0000
1.9000	2.2064	.7856	.8919	1.0000	.0000
1.9500	2.6001	.7690	.9955	1.0000	-.0000
2.0000	3.0906	.7535	1.1276	1.0327	-.0327
2.0500	3.7207	.7395	1.3012	******	******
2.1000	4.5557	.7273	1.5305	******	******
2.1500	5.7202	.7168	1.8717	1.0000	.0000
2.2000	7.4414	.7083	2.3768	R	-R
2.2500	10.2332	.7017	3.2242	R	-R

PERMITTIVITY = 2.56

DIAMETER FACTOR = 1.00

Z1	Z2	LAMBDA G / LAMBDA 3	DIAMETER / LAMBDA 0	FRACTIONAL INTERNAL ENERGY	FRACTIONAL EXTERNAL ENERGY
1.0000	.0517	.9979	.2552	.0322	.9678
1.0500	.0730	.9963	.2682	.0525	.9475
1.1000	.0991	.9938	.2815	.0794	.9206
1.1500	.1301	.9903	.2950	.1128	.8872
1.2000	.1666	.9856	.3088	.1525	.8475
1.2500	.2086	.9795	.3230	.1978	.8022
1.3000	.2573	.9718	.3377	.2477	.7523
1.3500	.3127	.9625	.3532	.3014	.6986
1.4000	.3758	.9514	.3694	.3578	.6422
1.4500	.4478	.9383	.3868	.4159	.5841
1.5000	.5298	.9232	.4054	.4748	.5252
1.5500	.6236	.9064	.4258	.5336	.4664
1.6000	.7313	.8875	.4483	.5914	.4086
1.6500	.8557	.8669	.4737	.6473	.3527
1.7000	1.0006	.8447	.5027	.7008	.2992
1.7500	1.1705	.8214	.5366	.7509	.2491
1.8000	1.3719	.7973	.5768	.7973	.2027
1.8500	1.6136	.7729	.6256	.8392	.1608
1.9000	1.9070	.7489	.6861	.8763	.1237
1.9500	2.2687	.7260	.7624	.9081	.0919
2.0000	2.7246	.7047	.8614	.9346	.0654
2.0500	3.3142	.6855	.9932	.9560	.0440
2.1000	4.0942	.6689	1.1727	.9721	.0279
2.1500	5.1855	.6550	1.4306	.9839	.0161
2.2000	6.8115	.6439	1.8242	.9918	.0082
2.2500	9.4629	.6354	2.4789	.9965	.0035

PERMITTIVITY = 2.56

DIAMETER FACTOR = 2.00

Z1	Z2	LAMBDA G / LAMBDA 0	DIAMETER / LAMBDA 0	FRACTIONAL INTERNAL ENERGY	FRACTIONAL EXTERNAL ENERGY
1.0000	.0517	.9979	.2552	.0934	.9066
1.0500	.0730	.9963	.2662	.1456	.8544
1.1000	.0991	.9938	.2815	.2101	.7899
1.1500	.1301	.9903	.2950	.2845	.7155
1.2000	.1666	.9856	.3088	.3657	.6343
1.2500	.2088	.9795	.3230	.4501	.5499
1.3000	.2573	.9718	.3377	.5343	.4657
1.3500	.3127	.9625	.3532	.6152	.3848
1.4000	.3758	.9514	.3694	.6903	.3097
1.4500	.4478	.9383	.3868	.7578	.2422
1.5000	.5298	.9233	.4054	.8165	.1835
1.5500	.6236	.9064	.4258	.8659	.1341
1.6000	.7313	.8875	.4483	.9059	.0941
1.6500	.8557	.8669	.4737	.9370	.0630
1.7000	1.0006	.8447	.5027	.9602	.0398
1.7500	1.1705	.8214	.5366	.9765	.0235
1.8000	1.3719	.7973	.5768	.9873	.0127
1.8500	1.6136	.7729	.6256	.9938	.0062
1.9000	1.9070	.7489	.6861	.9973	.0027
1.9500	2.2667	.7260	.7624	.9990	.0010
2.0000	2.7246	.7047	.8614	.9997	.0003
2.0500	3.3142	.6855	.9932	.9999	.0001
2.1000	4.0942	.6689	1.1727	1.0000	.0000
2.1500	5.1855	.6550	1.4306	1.0000	.0000
2.2000	6.8115	.6438	1.8242	1.0000	.0000
2.2500	9.4629	.6354	2.4789	1.0000	-.0000

PERMITTIVITY = 2.56

DIAMETER FACTOR = 5.00

Z1	Z2	LAMBDA G / LAMBDA 0	DIAMETER / LAMBDA 0	FRACTIONAL INTERNAL ENERGY	FRACTIONAL EXTERNAL ENERGY
1.0000	.0517	.9979	.2552	.2846	.7154
1.0500	.0730	.9963	.2682	.4042	.5958
1.1000	.0991	.9938	.2815	.5284	.4716
1.1500	.1301	.9903	.2950	.6462	.3538
1.2000	.1666	.9856	.3088	.7490	.2510
1.2500	.2088	.9795	.3230	.8321	.1679
1.3000	.2573	.9718	.3377	.8944	.1056
1.3500	.3127	.9625	.3532	.9379	.0621
1.4000	.3758	.9514	.3694	.9661	.0339
1.4500	.4478	.9383	.3868	.9829	.0171
1.5000	.5298	.9233	.4054	.9921	.0079
1.5500	.6236	.9064	.4258	.9968	.0032
1.6000	.7313	.8875	.4483	.9988	.0012
1.6500	.8557	.8669	.4737	.9996	.0004
1.7000	1.0006	.8447	.5027	.9999	.0001
1.7500	1.1705	.8214	.5366	1.0000	.0000
1.8000	1.3719	.7973	.5768	1.0000	.0000
1.8500	1.6136	.7729	.6256	1.0000	.0000
1.9000	1.9070	.7489	.6861	1.0000	.0000
1.9500	2.2687	.7260	.7624	1.0000	.0000
2.0000	2.7246	.7047	.8614	1.0000	.0000
2.0500	3.3142	.6855	.9932	1.0000	.0000
2.1000	4.0942	.6689	1.1727	1.0000	-.0000
2.1500	5.1855	.6550	1.4306	.9998	.0002
2.2000	6.8115	.6438	1.8242	1.0000	.0000
2.2500	9.4629	.6354	2.4789	******	******

PERMITTIVITY = 2.56

DIAMETER FACTOR =10.00

Z1	Z2	LAMBDA G / LAMBDA 0	DIAMETER / LAMBDA 0	FRACTIONAL INTERNAL ENERGY	FRACTIONAL EXTERNAL ENERGY
1.0000	.0517	.9979	.2552	.5452	.4548
1.0500	.0730	.9963	.2682	.6943	.3057
1.1000	.0991	.9938	.2815	.8141	.1859
1.1500	.1301	.9903	.2950	.8983	.1017
1.2000	.1666	.9856	.3088	.9501	.0499
1.2500	.2088	.9795	.3230	.9783	.0217
1.3000	.2573	.9718	.3377	.9916	.0084
1.3500	.3127	.9625	.3532	.9972	.0028
1.4000	.3758	.9514	.3694	.9992	.0008
1.4500	.4478	.9383	.3868	.9998	.0002
1.5000	.5298	.9233	.4054	1.0000	.0000
1.5500	.6236	.9064	.4258	1.0000	.0000
1.6000	.7313	.8875	.4483	1.0000	.0000
1.6500	.8557	.8669	.4737	1.0000	.0000
1.7000	1.0006	.8447	.5027	1.0000	.0000
1.7500	1.1705	.8214	.5366	1.0000	.0000
1.8000	1.3719	.7973	.5768	1.0000	.0000
1.8500	1.6136	.7729	.6256	1.0000	-.0000
1.9000	1.9070	.7489	.6861	1.0000	-.0000
1.9500	2.2687	.7260	.7624	1.0000	.0000
2.0000	2.7246	.7047	.8614	1.0000	-.0000
2.0500	3.3142	.6855	.9932	4.4012	******
2.1000	4.0942	.6689	1.1727	******	******
2.1500	5.1855	.6550	1.4306	******	******
2.2000	6.8115	.6438	1.8242	R	-R
2.2500	9.4629	.6354	2.4789	R	-R

NSWC/WOL TR 77-115

PERMITTIVITY = 3.78

DIAMETER FACTOR = 1.00

Z1	Z2	LAMBDA G / LAMBDA 0	DIAMETER / LAMBDA 0	FRACTIONAL INTERNAL ENERGY	FRACTIONAL EXTERNAL ENERGY
1.0000	.0177	.9996	.1909	.0065	.9935
1.0500	.0277	.9990	.2005	.0132	.9868
1.1000	.0411	.9981	.2101	.0242	.9758
1.1500	.0582	.9965	.2198	.0406	.9594
1.2000	.0795	.9940	.2296	.0634	.9366
1.2500	.1052	.9904	.2395	.0930	.9070
1.3000	.1358	.9853	.2495	.1296	.8704
1.3500	.1718	.9786	.2598	.1731	.8269
1.4000	.2139	.9697	.2704	.2228	.7772
1.4500	.2629	.9585	.2813	.2779	.7221
1.5000	.3197	.9446	.2928	.3373	.6627
1.5500	.3859	.9276	.3049	.3999	.6001
1.6000	.4633	.9072	.3180	.4643	.5357
1.6500	.5544	.8832	.3323	.5294	.4706
1.7000	.6626	.8554	.3483	.5939	.4061
1.7500	.7924	.8239	.3667	.6566	.3434
1.8000	.9503	.7891	.3886	.7166	.2834
1.8500	1.1451	.7516	.4154	.7727	.2273
1.9000	1.3889	.7128	.4493	.8238	.1762
1.9500	1.6988	.6743	.4937	.8690	.1310
2.0000	2.0993	.6379	.5535	.9073	.0927
2.0500	2.6257	.6055	.6360	.9381	.0619
2.1000	3.3362	.5782	.7526	.9616	.0384
2.1500	4.3359	.5563	.9239	.9783	.0217
2.2000	5.8154	.5398	1.1870	.9891	.0109
2.2500	8.2471	.5280	1.6320	.9955	.0045

PERMITTIVITY = 3.78

DIAMETER FACTOR = 2.00

Z1	Z2	LAMBDA G / LAMBDA 0	DIAMETER / LAMBDA 0	FRACTIONAL INTERNAL ENERGY	FRACTIONAL EXTERNAL ENERGY
1.0000	.0177	.9996	.1909	.0208	.9792
1.0500	.0277	.9990	.2005	.0406	.9594
1.1000	.0411	.9981	.2101	.0711	.9289
1.1500	.0582	.9965	.2198	.1139	.8861
1.2000	.0795	.9940	.2296	.1691	.8309
1.2500	.1052	.9904	.2395	.2358	.7642
1.3000	.1358	.9853	.2495	.3120	.6880
1.3500	.1718	.9786	.2598	.3947	.6053
1.4000	.2139	.9697	.2704	.4804	.5196
1.4500	.2629	.9585	.2813	.5659	.4341
1.5000	.3197	.9446	.2928	.6478	.3522
1.5500	.3859	.9276	.3049	.7234	.2766
1.6000	.4633	.9072	.3180	.7907	.2093
1.6500	.5544	.8832	.3323	.8484	.1516
1.7000	.6626	.8554	.3483	.8957	.1043
1.7500	.7924	.8239	.3667	.9326	.0674
1.8000	.9503	.7891	.3886	.9597	.0403
1.8500	1.1451	.7516	.4154	.9783	.0217
1.9000	1.3889	.7128	.4493	.9897	.0103
1.9500	1.6988	.6743	.4937	.9959	.0041
2.0000	2.0993	.6379	.5535	.9987	.0013
2.0500	2.6257	.6055	.6360	.9997	.0003
2.1000	3.3362	.5782	.7526	1.0000	.0000
2.1500	4.3359	.5563	.9239	1.0000	.0000
2.2000	5.8154	.5398	1.1870	1.0000	.0000
2.2500	8.2471	.5280	1.6320	1.0000	.0000

PERMITTIVITY = 3.78

DIAMETER FACTOR = 5.00

Z1	Z2	LAMBDA G / LAMBDA D	DIAMETER / LAMBDA G	FRACTIONAL INTERNAL ENERGY	FRACTIONAL EXTERNAL ENERGY
1.0000	.0177	.9996	.1909	.0760	.9240
1.0500	.0277	.9990	.2065	.1380	.8620
1.1000	.0411	.9981	.2101	.2231	.7769
1.1500	.0582	.9965	.2198	.3275	.6725
1.2000	.0795	.9940	.2296	.4436	.5564
1.2500	.1052	.9904	.2395	.5619	.4381
1.3000	.1358	.9853	.2495	.6730	.3270
1.3500	.1718	.9786	.2598	.7696	.2304
1.4000	.2139	.9697	.2704	.8475	.1525
1.4500	.2629	.9585	.2813	.9059	.0941
1.5000	.3197	.9446	.2928	.9462	.0538
1.5500	.3859	.9276	.3049	.9719	.0281
1.6000	.4633	.9072	.3180	.9868	.0132
1.6500	.5544	.8832	.3323	.9945	.0055
1.7000	.6626	.8554	.3483	.9980	.0020
1.7500	.7924	.8239	.3667	.9994	.0006
1.8000	.9503	.7891	.3886	.9999	.0001
1.8500	1.1451	.7516	.4154	1.0000	.0000
1.9000	1.3889	.7128	.4493	1.0000	.0000
1.9500	1.6988	.6743	.4937	1.0000	.0000
2.0000	2.0993	.6379	.5535	1.0000	.0000
2.0500	2.6257	.6055	.6360	1.0000	.0000
2.1000	3.3362	.5782	.7526	1.0000	-.0000
2.1500	4.3359	.5563	.9239	1.0000	-.0000
2.2000	5.8154	.5398	1.1870	1.0348	-.0348
2.2500	8.2471	.5280	1.6320	******	******

PERMITTIVITY = 3.78

DIAMETER FACTOR =10.00

Z1	Z2	LAMBDA G / LAMBDA 0	DIAMETER / LAMBDA 0	FRACTIONAL INTERNAL ENERGY	FRACTIONAL EXTERNAL ENERGY
1.0000	.0177	.9996	.1909	.1835	.8165
1.0500	.0277	.9990	.2005	.3063	.6937
1.1000	.0411	.9981	.2101	.4513	.5487
1.1500	.0582	.9965	.2198	.5997	.4003
1.2000	.0795	.9940	.2296	.7328	.2672
1.2500	.1052	.9904	.2395	.8380	.1620
1.3000	.1358	.9853	.2495	.9114	.0886
1.3500	.1718	.9786	.2598	.9567	.0433
1.4000	.2139	.9697	.2704	.9813	.0187
1.4500	.2629	.9585	.2813	.9930	.0070
1.5000	.3197	.9446	.2928	.9977	.0023
1.5500	.3859	.9276	.3049	.9994	.0006
1.6000	.4633	.9072	.3180	.9999	.0001
1.6500	.5544	.8832	.3323	1.0000	.0000
1.7000	.6626	.8554	.3483	1.0000	.0000
1.7500	.7924	.8239	.3667	1.0000	.0000
1.8000	.9503	.7891	.3886	1.0000	.0000
1.8500	1.1451	.7516	.4154	1.0000	.0000
1.9000	1.3889	.7128	.4493	1.0000	.0000
1.9500	1.6988	.6743	.4937	1.0000	-.0000
2.0000	2.0993	.6379	.5535	1.0000	-.0000
2.0500	2.6257	.6055	.6360	1.0000	-.0000
2.1000	3.3362	.5782	.7526	4.7228	******
2.1500	4.3359	.5563	.9239	1.0000	.0000
2.2000	5.8154	.5398	1.1870	R	-R
2.2500	8.2471	.5280	1.6320	R	-R

NSWC/WOL TR 77-115

DISTRIBUTION

Commander
Naval Air Systems Command
Washington, DC 20360
J. W. Willis (310B)
E. T. Hooper (370D)
A. Glista (52022G)

Commander
Naval Weapons Center
China Lake, CA 93555
J. Blair (2608)
R. P. Moore (3542)
Technical Library

Commander
Naval Sea Systems Command
Washington, DC 20362
T. Tasaka (NSEA 03415)
M. Wapner (NSEA 0341)

Commander
Naval Air Development Center
Johnsville, PA 18974
M. Foral (2042)
Technical Library

Director
Naval Research Laboratory
Washington, DC 20375
B. Spielman
C. Vittoria

Commanding Officer
Naval Avionics Center
Indianapolis, IN 46218
R. Katz (D813)

Commander
Naval Electronics Systems Command
Washington, DC 20360
C. Rigdon (30422)
M. Siegmann (30432)
E. Maynard (30433)

Commander
Naval Ocean Systems Center
San Diego, CA 92152
D. Rubin
D. Marcus

DISTRIBUTION (Cont.)

Commanding Officer
Harry Diamond Laboratories
Adelphi, MD 20783
Howard Jones

Commanding Officer
U.S. Army Electronics Command
Fort Monmouth, NJ 07703
H. Jacobs (AMSEL-TL-IJ)

Commanding Officer
SAMSO/RSMG
Air Force Systems Command
Los Angeles, CA 90009
J. P. Rouge

Epsilon Lambda
28 S. Water Street
Batavia, IL 60510
R. Knox

Ball Brothers Research Corp.
P.O. Box 1062
Boulder, CO 80302
L. T. Ostwald

Defense Documentation Center
Cameron Station
Alexandria, VA 22314 12